Nuclear Emulsion Technique*

ARTHUR BEISER

New York University, University Heights, New York, New York

TABLE OF CONTENTS

Chapter 1. Properties of Nuclear Emulsions

1–1. INTRODUCTION

A PHOTOGRAPHIC emulsion is merely, as Yagoda has put it, "a cleverly contrived mixture of silver bromide dispersed in an extract of cowhide." Nuclear emulsions are photographic emulsions of very high silver concentration that are thickly coated on glass backings. Ionizing particles which happen to pass through such emulsions leave behind a number of silver bromide crystals that have been so altered that, upon development, they appear as rows of black grains of colloidal silver and identify the trajectories of the particles. The more strongly ionizing the particles, the more numerous are these grains; and the greater their initial energies, the longer the resulting tracks. Relationships exist which connect these quantities very accurately, enabling the identification of the involved particle and its energy under favorable circumstances. More elaborate methods, for example, those making use of the multiple small-angle scattering of light particles, can be used in the event that range and grain density measurements are not adequate in a particular case. Auxiliary techniques, such as those utilizing the deflection of charged particles in an intense magnetic field, are frequently of value in specialized applications.

The first use of photographic emulsions in recording particle tracks was made by Reinganum† (1911), who found that alpha-particles could render developable several of the silver bromide grains along their paths in an emulsion. His work, which occurred at about the same time that C. T. R. Wilson successfully photographed cloud-chamber tracks, was based in part upon the discovery the previous year (Kinoshita, 1910) that alpha-particles could produce developability in individual bromide grains. Michl (1912) performed the first quantitative evaluations of these alpha-particle tracks. It was not until 1925 that proton tracks were observed in an emulsion, this having been accomplished by M. Blau (1925), who, with H. Wambacher, did much of the pioneering research in nuclear emulsions. The early history of the photographic detection of nuclear particles was outlined by Shapiro (1941).

Emulsions manufactured especially for these purposes were introduced by Ilford Ltd., the first being the R1 plates sensitive only to alpha-particles, which were followed by the R2 plates that could record low energy proton tracks (Taylor, 1935) and the even more sensitive "Halftone" emulsions. The performance of the Ilford series was improved upon by Agfa with their K plates (Wambacher, 1939). Eastman Kodak, in collaboration with T. R. Wilkins, produced the "Fine Grain Alpha-Plates" at about this same time.

During and since the war enormous advances have been made in nuclear emulsion manufacture and techniques, to a great extent the result of the efforts of C. F. Powell of the University of Bristol and his coworkers. The development by Kodak Ltd. in 1948 of the NT4 emulsions, sensitive to all charged particles regardless of energy, and the discovery of the meson decay scheme immediately before represent the mat-

* The preparation of this paper was assisted in part by the joint program of the ONR and AEC.

† An alphabetic bibliography is given at the end of this paper.

TABLE 1-I. The compositions of dry Ilford, Kodak Ltd., and Eastman Kodak nuclear emulsions in grams/centimeter³.

Element	Ilford	Kodak Ltd.	Eastman Kodak
Silver	2.025	1.97	1.70
Bromine	1.465	1.44	1.22
Iodine	0.057	0.036	0.054
Carbon	0.30	0.27	0.34
Hydrogen	0.049	0.038	0.043
Oxygen	0.20	0.16	0.17
Sulfur	0.011	...	...
Nitrogen	0.073	0.080	0.11

uration of the photographic method. In the relatively short period since then the area of usefulness of nuclear emulsions has been continually broadened until their position as an important research tool in nuclear physics is now well established.

1-2. CHARACTERISTICS OF EMULSIONS

Physical Properties

Nuclear emulsions are manufactured commercially by Ilford Ltd. and Kodak Ltd. in England and by the Eastman Kodak Company in the United States. The compositions of these emulsions in terms of the number of grams of each element present per cubic centimeter of completely dry emulsion are given in Table 1–I, and in terms of the number of atoms per cubic centimeter of emulsion in Table 1–II. For Ilford G5 emulsions the bromine and iodine contents are 1.496 and 0.026 g/cm³, respectively. The figures for the Eastman Kodak emulsions do not include their type NTC, which has a much lower silver halide content (65 percent) than do their others (81 percent). Gelatin is hygroscopic, and hence the emulsion compositions will vary with atmospheric humidity. The percentage moisture contents by weight of the different emulsions under various relative humidities at a temperature of 20°C are given in Table 1–III.

Nuclear emulsions manufactured by the above companies are normally supplied coated on glass plates 1.25 to 1.40 mm thick, with emulsion thicknesses of from 25 to 600 microns regularly available in most cases. Greater and smaller thicknesses may be obtained on special order. Plate sizes range from 1 by 3 inches to a maximum of perhaps 8 by 10 inches, with the smaller sizes permitting microscopic examination without further cutting. Emulsions are also supplied unsupported as pellicles, the use of which enables relatively prolonged exposure in vacuum without damage and also affords a degree of flexibility. A solid block of emulsion may be approximated by packing a number of pellicles together, which may be subsequently separated and developed individually. The pellicles are usually mounted on glass plates after processing to facilitate their study.

TABLE 1-II. The compositions of dry Ilford, Kodak Ltd., and Eastman Kodak nuclear emulsions in atoms/centimeter³ $\times 10^{22}$.

Element	Ilford	Kodak Ltd.	Eastman Kodak
Silver	1.17	1.14	0.99
Bromine	1.15	1.13	0.96
Iodine	0.03	0.02	0.027
Carbon	1.51	1.43	1.60
Hydrogen	2.93	2.39	2.64
Oxygen	0.75	0.65	0.68
Sulfur	0.02	...	...
Nitrogen	0.31	0.36	0.49

The surfaces of these emulsions are extremely sensitive to pressure (Mather, 1948), but the presence of a thin surface coating of gelatin will prevent most abrasion marks from being formed. Eastman Kodak supplies 0.5- to 1-micron coatings on its plates upon request. When particles are incident from the surface, such coatings will decrease their ranges by a small amount which may be corrected for (Mauer and Reynolds, 1948). Ilford also supplies emulsions with super coating.

Sensitivities

The sensitivities of nuclear emulsions are conveniently expressed in terms of the maximum detectable energies of various particles in them. Tables 1–IV, 1–V, and 1–VI give the sensitivities of Ilford, Kodak Ltd., and Eastman Kodak emulsions on this basis for electrons, μ-mesons, protons, deuterons, and alpha-particles.

TABLE 1-III. The percentage moisture contents by weight of Ilford, Kodak Ltd., and Eastman Kodak nuclear emulsions at various relative humidities at 20°C.

% Relative humidity	Ilford	Kodak Ltd.	Eastman Kodak
0	1.41	...	...
30	2.06	1.3	...
50	2.65	2.6	2.2
60	2.95	...	...
70	3.7	3.5	4.0
85	5.17	...	...

Preparation of Nuclear Emulsions

Although it is usually possible to obtain suitable commercially manufactured nuclear emulsions, details of their laboratory preparation are nevertheless of interest. Early emulsions were prepared by Myssowsky and Tschijow (1927), Blau and Wambacher (1932), and Jdanoff (1935), while the more recent work of Demers (1946, 1947), Hälg and Jenny (1948), and Jenny (1951) has resulted in workable formulas for making emulsions of high sensitivity. Ilford supplies the G5 emulsion in liquid form for work requiring extremely fresh emulsion, since plates can be coated immediately before use.

Jdanoff (1935) has shown on the basis of geometrical considerations that the mean grain density $\langle dn/dx \rangle$ of a track in an emulsion of silver halide concentration C and density ρ is

$$\langle dn/dx \rangle = (\tfrac{3}{2})(CP/\rho d), \qquad (1\text{-}1)$$

where d is the average grain diameter and P the probability for a given specific energy loss that traversal of a grain will render it developable. It would seem from this equation that increasing C and decreasing d would result in emulsions characterized by high

grain densities, a very desirable feature. However, the factors involved in Eq. (1-1) are not all independent, since it is known that P is approximately proportional to d^3. Hence reducing d will diminish P to an even greater extent, and it is necessary to make a more or less arbitrary compromise at some point. If the recording of weakly ionizing particles is desired, the compromise should be in favor of a high P, since such particles will otherwise escape detection. Low energy particles, on the other hand, ionize heavily but have very short tracks. In such cases it is desirable to decrease d in order that the range be accurately defined.

Demers' Technique

The first emulsions made by Demers (1945) were of relatively low sensitivity, resulting, for example, in a grain density of about 50 grains per 100 microns for 7–8 Mev proton tracks. These emulsions were prepared by simultaneously adding 30 ml of a 60 percent silver nitrate solution and 30 ml of a 42 percent potassium bromide solution to 75 ml of 6 percent gelatin solution. The operation is carried out at a temperature of from 40° to 50°C, and the silver and bromide solutions are added dropwise over a period of 30 minutes with constant stirring. This emulsion must be washed in cold water for several hours and then dried. Most of the resulting bromide grains are less than 0.2 micron in diameter, with slightly larger sizes resulting from the use of lower temperatures or slower stirring. Such emulsions are not very light-sensitive and so may be prepared under a red or amber darkroom safelight.

Later investigations by Demers (1947) have resulted in an improved emulsion. A solution of 4.5 g of gelatin in 50 ml of water is first prepared, and 25 ml of ethyl alcohol added. The function of the alcohol is to prevent clumps and large grains from forming. Solutions of 18.6 g silver nitrate in 30 ml water and 12.8 g potassium bromide in 30.5 ml water are then added simultaneously under the same conditions as above. A slight excess of the bromide is desirable during the process, this condition being obtained by allowing 0.5 to 1 ml of bromide solution to flow before starting the addition of silver nitrate. The resulting emulsion is poured into a flat tray and cooled until it jells, with about 8 hours of washing then being required to remove the soluble potassium nitrate. The emulsion may then be melted and coated on appropriate glass plates.

TABLE 1-IV. The maximum detectable energies in Mev of various particles in Ilford nuclear emulsions.

Particle	D1	E1	C2	B2	G5
Electron	...	...	0.03	0.07	all
μ-Meson	...	2	5.5	0.14	all
Proton	...	20	50	120	all
Deuteron	...	40	100	240	all
Alpha-particle	low	500	1500	all	all

Hälg and Jenny's Technique

Hälg and Jenny (1948), elaborating on Demers' procedure, have provided a more detailed method for making emulsions. They employ a solution of mixed bromide and iodide prepared by adding 5 ml of 10 percent $CdBr_2(4H_2O)$ and 2 ml of 10 percent KI to 14 g of KBr in 23 ml of water. This solution and 30 ml of a 60 percent silver nitrate solution are added at a rate of about 1 ml per minute to a gelatin solution. The latter is prepared by first soaking 6.5 g gelatin in 70 ml water at 20°C for about an hour and then dissolving it by heating to 50°C and stirring. After the silver and halide solutions have been added the emulsion is ripened at the same temperature for 45 minutes, and then poured into a porcelain dish and cooled on ice for 6 hours. The resulting gel is cut into pieces and washed in cheesecloth until free from potassium nitrate, which requires perhaps 16 hours. Two further solutions must now be prepared, the first containing 2 g chrome alum in 78 ml water to which is added 60 ml ethyl alcohol, 42 ml glycerine and 0.75 ml of 10 percent potassium bromide. The washed emulsion is melted at 35°C and 9 ml of this solution and 5 ml of a 0.2 percent wetting agent added. The further addition of 1 ml of a 2 percent solution of acridine orange, a sensitizing dye, will improve the emulsion characteristics. The second solution, composed of 2 g gelatin dissolved in 150 ml water at 35°C, 5 ml of the wetting agent, and 2.5 ml of 2 percent chrome alum, after filtration, is used as a preliminary coating on the glass backings to be used. About 1 ml per 1- by 3-inch plate is required. When this has hardened the melted emulsion is poured on and the resulting plates cooled until it sets. Filtered air is desirable for drying.

TABLE 1-V. The maximum detectable energies in Mev of various particles in Kodak Ltd. nuclear emulsions.

Particle	NT1a	NT2a	NT4
Electron	...	0.1	all
μ-Meson	2	20	all
Proton	20	200	all
Deuteron	40	400	all
Alpha-particle	500	all	all

Jenny (1951) has produced electron-sensitive emulsions in his laboratory, but his formula involves the use of specially treated gelatin manufactured in Switzerland which includes various chemical sensitizers. The sensitivity and grain size are greatly increased in this method by adding a small volume of concentrated ammonia to the emulsion while ripening, after 5 minutes the ammonia being neutralized with citric acid. This treatment was found to increase emulsion sensitivity by a factor of 3.

1-3. TEMPERATURE VARIATION OF SENSITIVITY

The sensitivity of nuclear emulsions varies considerably with the temperature when exposed. This variation has been experimentally investigated by several authors (Dilworth, 1949; Dollmann, 1950; Lord, 1951) in terms of the total number of developed grains in tracks of monoenergetic protons exposed at various temperatures. A summary of the results of Dollmann and Lord appears in Fig. 1-1. The work of Dilworth, confined to low temperatures, is in agreement with these curves.

An empirical relationship governing the variation of the grain density with exposure temperature has been found by Beiser (1951). This is

$$n = A \exp(-\epsilon_1/kT)[1 - a \exp(-\epsilon_2/kT)], \quad (1\text{–}2)$$

where n is the grain density, T the exposure temperature, A a function of the sensitivity of the emulsion and of the rate of energy loss of the particle producing the

TABLE 1-VI. The maximum detectable energies in Mev of various particles in Eastman Kodak nuclear emulsions.

Particle	NTC	NTC3	NTA	NTB	NTB2	NTB3
Electron	...	...	...	0.03	0.2	0.4
μ-Meson	...	1	2	6	40	85
Proton	...	1.5	3	8	50	110
Deuteron	...	20	40	100	750	1500
Alpha-particle	low	100	200	800	all	all

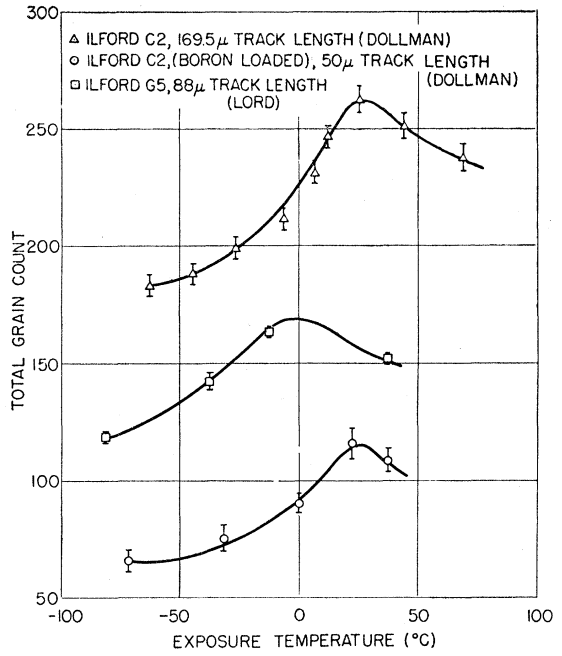

FIG. 1–1. Temperature variation of the sensitivity of various nuclear emulsions (Dollmann, 1950; Lord, 1951).

track, and a, ϵ_1, and ϵ_2 constants depending on the emulsion. The first exponential may be interpreted as being proportional to the rate of arrival of silver ions at the sensitivity specks during the exposure and the second as the relative number of ions released from the speck at the same time due to thermal ejection of some of the electrons there (*cf.* Sec. 2–1). The ions may move either into adjacent vacant Ag^+ lattice points or back into interstitial positions in the crystal.

A knowledge of this temperature dependence provides much useful information. The optimum exposure temperature for maximum sensitivity may be determined, occuring for emulsions in common use in the vicinity of 20°C. For emulsions employed at other temperatures the reduced sensitivity may be corrected for in interpreting the resulting tracks by consulting the above curves. Furthermore, the decrease in sensitivity at low temperatures permits the use of a thermal "shutter" which may be used to limit the sensitive time of an emulsion in applications where the continuous recording of phenomena is not desirable (Dilworth, 1949). Lord reports zero sensitivity at −200°C, and it is probable that the presence of tracks due to exposures at temperatures even somewhat above this would be unobservable over the fog background. That part of the background due to stray radiation may itself be diminished by storage at reduced temperatures (Cosyns *et al.*, 1949).

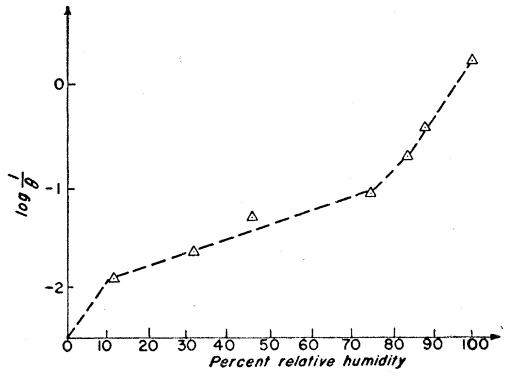

FIG. 1–2. The variation in θ, the time necessary for a reduction in grain density of one-half, with relative humidity (Albouy and Faraggi, 1949).

1–4. LATENT IMAGE FADING

The instability of the latent image in nuclear emulsions in the period between exposure and processing has been known since the early work by Blau (1931).

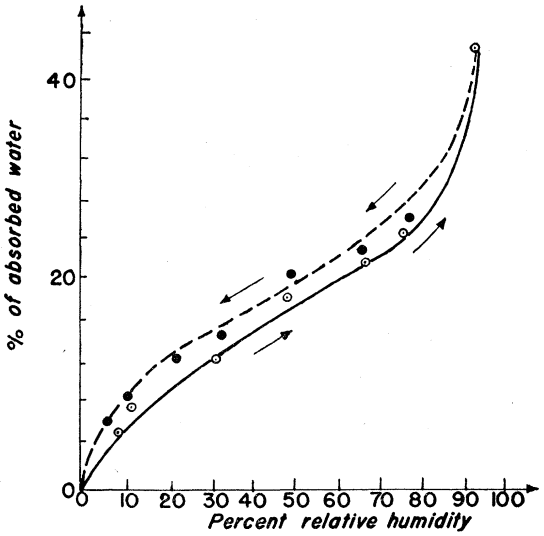

FIG. 1–3. The relation between the moisture absorbed by dry gelatin and the relative humidity (Mees, 1942).

This phenomenon is termed fading by analogy with the optical case, the grain density of a track gradually decreasing as a function of the time and conditions of storage. The effect of various parameters on fading will be discussed in the following in terms of the fading coefficient F, given by

$$F=(N-N_0)/N_0, \tag{1–3}$$

where N_0 is the number of grains in a given track length after immediate development and N the number after storage before development for a time t.

Atmosphere

Experiments by Mather (1949) indicate a reduction of about 90 percent in the fading of proton tracks when the irradiated emulsions are kept in a vacuum prior to development, showing that at least that proportion of

the fading phenomena is due to the action of some constituent or constituents of the atmosphere. Some or all of the residual fading may be explained (Beiser, 1950b) on the basis of the thermal ejection of electrons from the silver development centers of the latent image due to the acquisition of sufficient energy by these electrons to re-enter the conductance band of the crystal. Silver ions will then leave the speck, causing a reduction in its size sufficient in some cases to render it incapable of development.

The part played by the atmospheric humidity is extremely important. Albouy and Faraggi (1949) have investigated the variation in fading (here expressed in terms of θ, the time necessary for a reduction in grain density of one-half) with the relative humidity of the atmosphere surrounding the emulsion. Their results appear in Fig. 1–2. A comparison of this curve with the one given by Mees (1942), Fig. 1–3, showing the relation between the moisture absorbed by the gelatin of the emulsion and the relative humidity, indicates

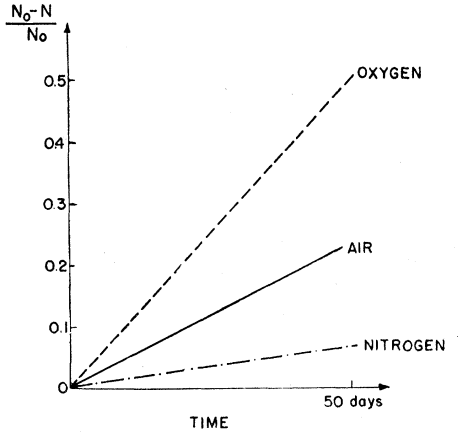

FIG. 1–4. The surface fading rates in Ilford C2 nuclear emulsions stored in various atmospheres at constant humidity (Albouy and Faraggi, 1949).

strongly that the rate of fading is an exponential function of the quantity of moisture retained by the gelatin.

Albouy and Faraggi have also examined the effect of varying the composition of the atmosphere surrounding the emulsions, maintaining the relative humidity constant. They find (Figs. 1–4 and 1–5) that the fading rate in pure oxygen is twice that in air and about ten times that in nitrogen. In every case, the fading is more rapid on the surface of the emulsion than it is in the interior.

Temperature

The variation of the fading rate with the temperature of storage may be determined (Beiser, 1951b) from a consideration of the effect of temperature on the velocity of a gas-solid chemical reaction, such as is assumed to occur during fading between certain constituents of the atmosphere and the silver development centers

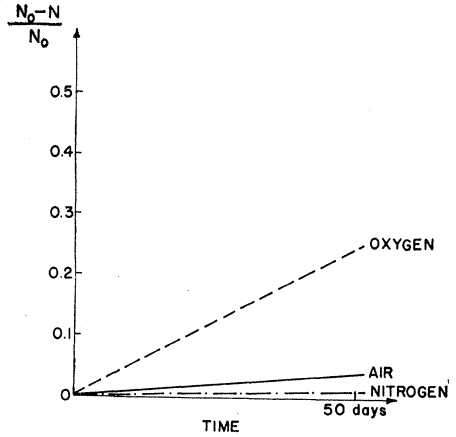

FIG. 1–5. The interior fading rates in Ilford C2 nuclear emulsions stored in various atmospheres at constant humidity (Albouy and Faraggi, 1949).

of the exposed emulsion. This gives a form of the Arrhenius relation, with $-dN/dt$ the rate of disappearance of the development centers, as the equation

$$-dN/dt = Ce^{-k/T}, \tag{1–4}$$

where T is the absolute temperature of storage and C and k constants. This implies that the fading produced under otherwise fixed conditions will be an exponential function of the reciprocal of the temperature, a result confirmed by the experiments of Albouy and Faraggi (1949).

Time

To obtain a relation between the magnitude of the latent image regression and the time of storage, the fading rate under a constant set of conditions may be considered proportional to the number of development

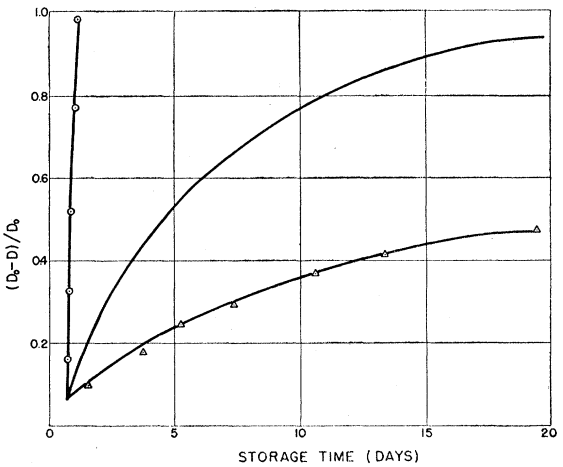

FIG. 1–6. The variation of the fading coefficient with time of storage under various conditions (Beiser, 1951b). Experimental points from Yagoda and Kaplan (1948). The upper curve refers to storage at saturation humidity, and the lower curve to normal laboratory conditions.

centers present (Beiser, 1951b). Since each of these is capable of producing a visible grain after development, this gives in integrated form

$$F=1-\exp(-ct). \tag{1-5}$$

The value of F is plotted in Fig. 1–6 as a function of t for various values of c, a constant dependent upon the emulsion and the storage conditions, in good agreement with the experimental values given by Yagoda and Kaplan (1948). In some cases (Wäffler and Younis, 1949) the fading is at first comparatively slow, corresponding to a small initial value for c, and then after a time increases rapidly, corresponding to a large c. LaPalme and Demers (1947) find that, in many cases, the grain spacing along a track increases according to an exponential law, which is in accordance with the treatment given above for F, the fading coefficient.

Emulsion Composition

Both the pH and the halide grain size affect the susceptibility of an emulsion to fading (Albouy and Faraggi, 1949). In general, the lower the pH and the smaller the grains the more rapid the fading. The impregnation of the emulsion with various substances (e.g., lithium, boron, uranium compounds) which have different pH values will alter the fading rate to extents dependent upon the amount of the difference. Since the sensitivity of a nuclear emulsion depends directly upon grain size, the larger grains having the greater sensitivity, plates such as the Ilford G5, Kodak NT4, and Eastman NTB3 suffer less from fading than do the others (Brown *et al.*, 1949).

Mechanism of Fading

The explanation of the fading mechanism proposed by Albouy and Faraggi (1949) appears on the basis of the available experimental evidence to be able to account for the approximately 90 percent of the effect due to the atmosphere. They suggest that fading is due to the oxidation of the development specks by atmospheric oxygen in the presence of water, the reaction proceeding as

$$\mathrm{Ag+O+H_2O\rightarrow 2Ag+2OH^-}. \tag{1-6}$$

It is evident that the presence of excess OH^- ions in the emulsion, i.e., pH values above 7, will act to inhibit the reaction, while more acid conditions accelerate it. The effect of humidity and oxygen concentration is obviously in accord with experiment.

Yagoda (1947, 1949) has proposed a hypothesis involving the oxidation of the specks by hydrogen peroxide produced in the emulsion in the immediate vicinity of the tracks by the action of the incident particles. That hydrogen peroxide is produced from water by ionizing radiation is known (Krenz, 1947), but a consideration of the quantities involved renders this explanation untenable.

Winand and Falla (1949) have suggested that rehalogenation of the silver atoms of the development centers by the bromide ions which surround them (Hautot, 1948) causes the fading. Since this theory cannot account for the effect of constituents of the atmosphere, it also must be discounted.

Chapter 2. Track Production and Evaluation

2-1. LATENT IMAGE FORMATION

The production of a latent (i.e., developable) image along the path of an ionizing particle in a nuclear emulsion is essentially the same process as that which occurs in an ordinary light-sensitive photographic emulsion. The only significant difference lies in the mechanism of ion pair formation; in the former case this occurs through the electrostatic interaction between the charged particle and the electrons of the emulsion atoms, and in the latter by the photoelectric emission of electrons by incident photons. Gurney and Mott (1938) provided the first comprehensive theory of the photolytic process, and, while modified subsequently by Mitchell (1948, 1949a,b) in a number of details, the fundamental concepts involved are well established.

According to the Gurney-Mott theory latent image formation occurs in two phases, one characterized by the motion of electrons within the silver bromide crystals and the other by the motion of ions. Initially, some of the electrons of the bromine ions have their energy states raised by the passage of the incident particle to vacant states in the conductance band of each crystal. These electrons then migrate freely through the crystal until they are trapped in places (sensitivity specks) characterized by localized energy levels below those of the conductance band. The sensitivity specks, actually clumps of silver or impurity atoms, are usually located on the crystal surface. The excess bromine diffuses slowly to the surface and is released there. The sensitivity specks, now negatively charged, attract interstitial silver ions (Frenkel defects) which are free to move through the crystal lattice, and these ions combine with the electrons there to form silver atoms. Silver specks of sufficient size to act as development centers are formed by repetitions of this process during the "exposure."

It is to be expected that latent image formation in nuclear emulsions is much less efficient in the utilization of the electrons resulting from an exposure than is true for photographic emulsions. Part of this inefficiency is a result of the short time needed for a particle to traverse each grain (Webb, 1948). For a 5-Mev alpha-particle and a 0.3-micron grain size this time is $\sim 2\times 10^{-14}$ second. Since the migration of the silver ions through the crystal is considerably slower than that of the electrons, the sensitivity specks acquire negative charges more rapidly than they can be neutralized, and further electrons are repelled until a sufficient number of silver ions reaches the specks. By that

time it is likely the other electrons will have been dispersed and have combined with silver ions at other points in the crystal, and the probability of any one speck being sufficiently sizeable to initiate development is correspondingly decreased. For weakly ionizing particles this effect should be relatively unimportant, a conclusion borne out by Berriman (1949), who finds that the efficiency, as defined above, for 50-kev electrons in Kodak Ltd. NT2a emulsions is comparable with that of light. This problem is discussed further in Sec. 2–2.

Development of an irradiated emulsion consists in the depositing of a sufficient number of additional silver atoms to render the crystal visible as a grain of colloidal silver. Photographic developers are weak reducing agents which require the presence of silver specks as catalysts for their action. Hence each silver bromide grain acts individually in development; if a sufficiently large latent image center exists in it, a grain will be entirely reduced, while if this is not the case it will not be affected at all. Subsequently the undeveloped grains are removed by a fixing bath, usually sodium thiosulfate, which facilitates the solution of silver bromide. The developed grains then remain embedded in the gelatin.

2–2. SPECIFIC ENERGY LOSS

The grain density of the track produced by a particle traversing a nuclear emulsion is usually measured in terms of the number of developed silver grains per unit path length. Alternatively, the reciprocal of this quantity, the mean grain spacing, may be employed, but the former is the preferred usage. In general, grain density depends upon the amount of ionization produced in the halide grains and upon their sensitivity, interpreted here as the number of electrons required to render each grain developable. Taking the sensitivity to be constant, the grain density is a function only of the specific energy loss of the incident particle, this loss being due principally to the excitation of the electrons of the stopping atoms by inelastic collisions.

Energy Loss

The average energy loss per unit distance $-dE/dx$ by collision processes has been given by Livingston and Bethe (1937) from a quantum-mechanical derivation as

$$\frac{-dE}{dx}=\frac{4\pi z^2e^4N}{mv^2}\left\{Z\left[\ln\left(\frac{2mv^2}{I}\right)-\ln(1-\beta^2)-\beta^2\right]-C_k\right\}, \tag{2–1}$$

where ze is the charge of the particle and v its velocity, N the number of atoms per cm^3 of the stopping material, Z and I their mean atomic number and ionization potential, respectively, m the electronic mass, $\beta=v/c$, and C_k a correction term required only in the event that v is comparable with the K electron velocities of the stopping atoms but large with respect to those of the other orbital electrons. For particles with velocities less than about 5×10^9 cm sec^{-1} the relativistic correction terms involving β nearly cancel and may be omitted, as is evident upon expanding $\ln(1-\beta^2)$ in a power series. According to Halliday (1950), for a 10-Mev alpha-particle in air $\ln(2mv^2/I)=5.1$, while the sum of the other two terms in the square brackets is only 4.5×10^{-4}. A further discussion of this equation has been given by Wheeler and Ladenburg (1941).

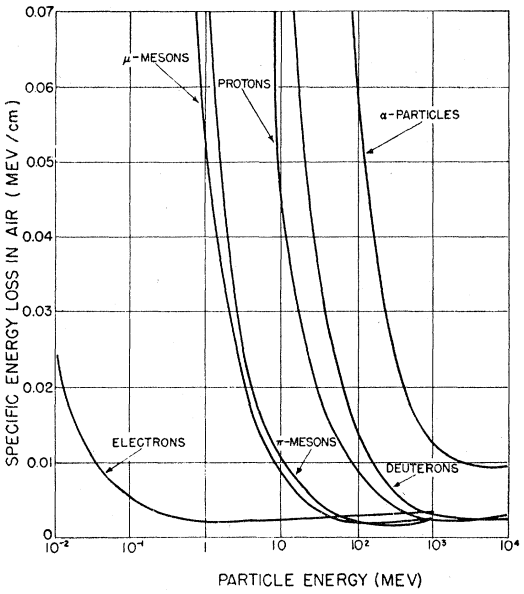

FIG. 2–1. Specific energy loss of various particles in air as a function of energy.

If v is fairly large, i.e., if $2mv^2/I>e$, where e is here the base of natural logarithms, the specific energy loss $-dE/dx$ will depend upon v according to the unbracketed term in Eq. (2–1). Thus $-dE/dx$ varies inversely with v^2 under such circumstances, and as a result the grain density of a track will increase in the direction of motion of the particle. At low energies (<1 Mev for protons and <0.1 Mev for alpha-particles) where the specific energy loss begins to decrease, Eq. (2–1) does not hold. This is a consequence of the lack of consideration given the random capture and loss of electrons at these velocities in deriving the expression. For example, a 0.8-Mev alpha-particle has an equal chance of being either singly or doubly charged at any time (Rutherford, 1924).

In Fig. 2–1 are shown the specific energy loss curves (according to Eq. (2–1)) for various particles as functions of energy, expressed in Mev per centimeter of air. To convert the curves to energy loss in an emulsion they must be multiplied by the stopping power of the emulsion relative to air (see Sec. 2–3). It is evident that all sufficiently energetic singly charged particles will have approximately the same energy loss minima,

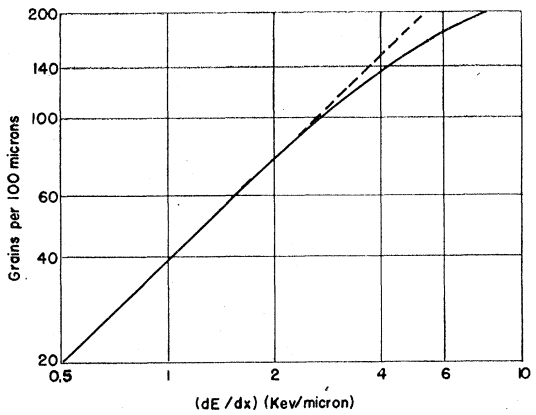

FIG. 2–2 Grain density in Ilford G5 emulsions as a function of specific energy loss (Fowler and Perkins, 1951).

with only slight increases at higher energies. The minimum grain densities recorded in nuclear emulsions of sufficient sensitivity will correspond to this quantity. The particle mass does not appear in Eq. (2–1), $-dE/dx$ being expressed in terms of its charge and velocity only, but in Fig. 2–1 $-dE/dx$ is plotted in terms of particle energy, which is a function of mass, and so the curves for each particle are displaced from each other although identical in shape. The minimum energy loss occurs for each particle at an energy of about $2m_0c^2$, where m_0 is its rest mass. The minimum energy for each is roughly 1 Mev for electrons, 200 Mev and 300 Mev for μ- and π-mesons, respectively, 2 Bev for protons, 4 Bev for deuterons, and 8 Bev for alpha-particles. Another point of interest is that, since the minimum specific energy loss for alpha-particles is four times that for singly charged particles, any track exhibiting less than four times minimum grain density must be due to one of the latter. Tracks with grain densities above four times minimum may, of course, be due to either, other methods of analysis being required for identification of the particle charge.

Grain Density

The measurement of the grain density of a track is a simple matter if the grains are discrete and if the fog background is not too great. The former condition results in an upper limit of perhaps 50 grains per 100 microns of track length, above this number many individual grains being unresolvable, and the latter a lower limit for visibility of perhaps 20 grains per 100 microns for a relatively low-background plate (less than 4 grains per micron^2). The curves of Fig. 4–11 in Sec. 4–8 give the precise values of the minimum grain densities for track recognition as functions of the background density. It is necessary to arbitrarily assign a grain count value n to unresolvable grain clumps, Fowler and Perkins (1951) taking $n=2.4l$, where l is the length of the clump in microns. In this connection it may be noted that the average developed grain diameter is about 0.3—0.4 micron.

It might be thought *a priori* that a direct proportionality exists between the specific energy losses of particles at various points on their trajectories and the corresponding grain densities. In Fig. 2–2 the number of developed silver grains per 100 microns of track length is plotted against the values of dE/dx in those intervals, the determinations having been made with Ilford G5 emulsions (Fowler and Perkins, 1951). It is evident that for high dE/dx values the proportionality relationship is no longer true, i.e., that emulsion sensitivity decreases for specific energy losses above a certain threshold. This is due to the inability of the sensitivity specks of the halide grains to acquire the electrons produced in their vicinity by the passage of a charged particle at a sufficiently rapid rate to prevent the formation of a space charge at high electron densities, with subsequent recombination and hence inefficiency of electron utilization (Sec. 2–1). For specific energy losses below a certain value the efficiency of electron utilization in terms of the proportion of electrons entering into the formation of a latent image relative to the number initially produced is more nearly constant, leading to the linearity of part of the curve in Fig. 2–2. For densities above 200 grains per 100 microns grain saturation occurs, and it is impossible to evaluate dE/dx for such tracks on the basis of grain counts since the proportionality between n and l ceases to hold for continuous grain distributions. Other methods for this purpose are available in certain cases, however, such as the evaluation of the delta-rays produced (Sec. 2–5).

According to the results of Debye and Hückel (1923) for strongly ionized electrolytes, the potential of an ion cloud surrounding an isolated ion is proportional to $N^{\frac{1}{2}}$, where N is the number of ions present. Taking

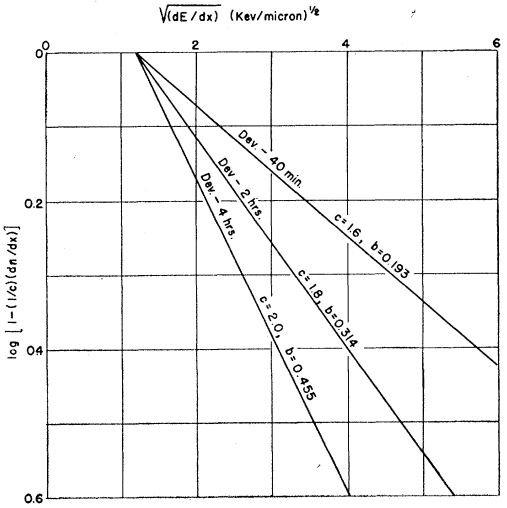

Fig. 2–3. A graphical representation of Eq. (2–3) relating specific energy loss and grain density (Morand and van Rossum, 1951).

into account that N is certainly proportional to dE/dx, Blau (1949) has given an expression for dn/dx, the grain density for singly charged particles, in the form

$$dn/dx = c\{1-\exp[-b(dE/dx)^{\frac{1}{2}}]\}, \qquad (2\text{–}2)$$

where b and c are experimentally determined constants dependent upon the emulsion under consideration and the processing technique employed. The numerical value of b for the unstated but presumably Ilford C2 emulsion results employed by Blau in her confirmation of Eq. (2–2) is $b=3$, although a slightly lower value, perhaps down as far as 2.5, might be more satisfactory in the low energy region. The value of c that was given was $c=4$. In this work x was measured in units of 0.85 micron. The constant b is a measure of the efficiency with which the liberated electrons due to the incident particle render the halide grains developable, and c is the maximum grain density possible in the emulsion, being approximately the number of halide grains per unit length present in the undeveloped emulsion.

A modification of the above relationship has been given by van Rossum (1949) and Morand and van Rossum (1951) as

$$dn/dx = c\{1-\exp[-bz(dE/dx)^{\frac{1}{2}}-a^{\frac{1}{2}}]\}. \qquad (2\text{–}3)$$

This equation results in even better agreement with the experimental results. The constant a is the minimum specific energy loss necessary to insure the developability of emulsion grains under the processing conditions employed. A plot of $\ln[1-(1/c)(dn/dx)]$ as a function of $(dE/dx)^{\frac{1}{2}}$ is shown in Fig. 2–3 for Ilford C3 boron-loaded plates developed in ID19 for various values of b and c, x being measured in microns and E in kev. The value of $a^{\frac{1}{2}}$ is given by the intersection of these curves with the abscissa and is 1.2 kev per micron here. Both b and c increase with increased development

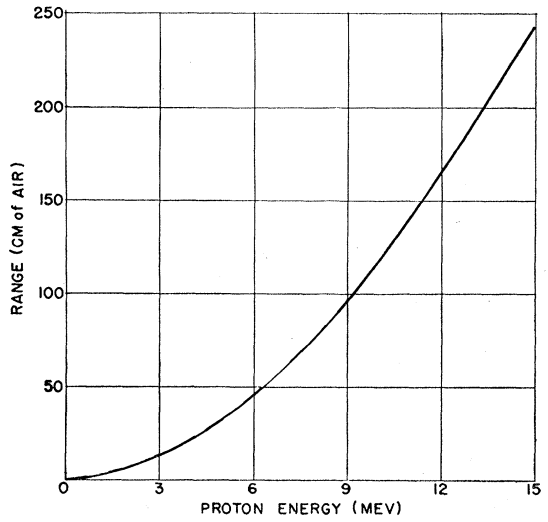

Fig. 2–4. Theoretical range-energy curve for protons in air to energies of 15 Mev (data from Livingston and Bethe, 1937).

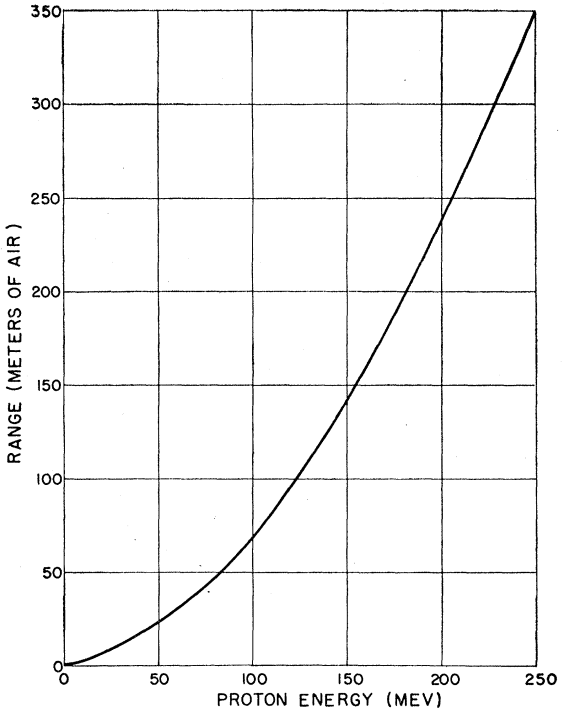

Fig. 2–5. Theoretical range-energy curve for protons in air to energies of 250 Mev (data from Smith, 1946).

time: Morand and van Rossum find that $b=0.314$ $M0.02$ and $c=1.8\pm0.1$ after two hours development at 5°C in ID19 diluted 1:3, and $b=0.455\pm0.02$ and $c=2.0\pm0.1$ after four hours. If fading has occurred, a will be increased in value and b and c decreased.

2–3. RANGE-ENERGY RELATIONSHIP

The energy loss of a charged particle in matter, although consisting of the loss of discrete amounts of energy in random collisions with electrons of the stopping substance, may be considered as a continuous process when taken over a finite path length. When the particle has come to a stop after traveling a distance R, its initial energy E will have been expended in the creation of ion pairs whose number is a function of E. Hence it is to be expected that there is a definite relationship between the energy and range of a given particle in a given stopping material, and the exact form of this relationship must be known in order to interpret range measurements in terms of the initial energies of the particles involved.

Theoretical Relationship

Knowing the specific energy loss dE/dx and initial energy E of an incident particle, the range is given by

$$R=\int_0^E dE/(dE/dx). \qquad (2\text{–}4)$$

TABLE 2-I. Range-energy relationship for protons and alpha-particles in Ilford B1 emulsions (measured to 13.0 Mev by Lattes *et al.*, 1947b, and extrapolated by Camerini and Lattes, 1947).

Energy Mev	Proton range microns	Alpha-particle range microns
0.5	5.5	2.1
1.0	14.5	3.52
1.5	26.0	4.96
2.0	40.0	6.54
2.5	56.5	8.34
3.0	75.0	10.38
3.5	97.0	12.60
4.0	120.5	15.0
4.5	146.0	17.65
5.0	173.0	20.5
5.5	202.0	23.6
6.0	234.0	26.7
6.5	269.0	30.0
7.0	306.0	33.6
7.5	345.0	37.5
8.0	385.0	41.4
8.5	426.0	45.3
9.0	469.0	49.5
9.5	515.0	53.7
10.0	564.0	58.0
10.5	614.0	62.6
11.0	666.0	67.7
11.5	720.0	72.7
12.0	776.0	77.8
12.5	834.0	83.4
13.0	895.0	...
15.0	1135	117
20.0	1870	201
25.0	2750	315
30.0	3760	464
35.0	4925	653

Livingston and Bethe (1937) have accurately evaluated this integral for protons in air up to energies of 15 Mev, and Smith (1946) has extended the computation to 10 Bev by using the equation

$$R=R(15)+\int_{15}^{E} dE/(dE/dx). \qquad (2\text{–}5)$$

Curves illustrating these theoretical results are given in Figs. 2–4 and 2–5. These determinations are based upon the assumption that the energy is expended in ionization and excitation of the stopping atoms exclusively, which is certainly approximately valid for energies below several hundred Mev. Above this point meson production becomes significant and Smith's values are of more restricted utility. These curves may be applied to nuclear emulsions by multiplying the range values by the stopping power of emulsion relative to air (see below).

TABLE 2-II. Experimental values of the range-energy relationship for protons in dry Ilford C2 emulsions (Bradner *et al.*, 1950).

Energy Mev	Range microns
7.8	389
16.4	1358
17.6	1465
22.3	2244
25.6	2849
28.2	3369
33.5	4597
39.5	6123

Combining Eqs. (2–1) and (2–4) gives

$$R=(M/z^2)f(v), \qquad (2\text{–}6)$$

where M is the mass, z the charge, and v the velocity of the particle. The quantity $f(v)$ does not depend upon either z or M. This equation is extremely useful as it enables the construction of range-energy curves for any ionizing particle when such a curve is known for one of a given mass and charge. Letting M_a, z_a and M_b, z_b refer to two different particles a and b of identical velocity in the same absorber, the relationship

$$R_b(v)=(z_a/z_b)^2(M_b/M_a)R_a(v) \qquad (2\text{–}7)$$

follows immediately. Of course

$$E_b=(M_b/M_a)E_a \qquad (2\text{–}8)$$

holds true. In addition,

$$(dE/dx)_{b,v}=(z_b/z_a)^2(dE/dx)_{a,v} \qquad (2\text{–}9)$$

permits transcribing energy loss figures, again for equal velocities. In terms of particles of the same energy, making use of Eq. (2–8) and enabling an immediate conversion of the curve for one to that of the others,

$$R_b(E)=(z_a/z_b)^2(M_b/M_a)R_a[(M_a/M_b)E], \qquad (2\text{–}10)$$

where $R_a[(M_a/M_b)E]$ is the range of a at an energy $[(M_a/M_b)E]$ and

$$(dE/dx)_{b,E}=(z_b/z_a)^2(dE/dx)_a[(M_a/M_b)E], \qquad (2\text{–}11)$$

where $(dE/dx)_a[(M_a/M_b)E]$ is the specific energy loss of a at an energy $[(M_a/M_b)E]$.

These relations are strictly true only when $z_a=z_b$, since the random capture and loss of electrons at low energies is identical for each particle in that case. In such a case Eqs. (2–7) to (2–11) are exact when experimental values are used for the reference particle, despite the fact that electron capture and loss was not considered in the derivation of Eq. (2–1). For protons and alpha-particles, however, the situation is different, with the experiments of Blackett and Lees (1932) giving

$$R_{\text{proton}}=(M_p/M_\alpha)(z_\alpha/z_p)^2R_\alpha-C, \qquad (2\text{–}12)$$

where $C=0.20$ cm air. It is obvious from Figs. 2–4 and 2–5 that a correction of this magnitude is significant only at very low energies. Since 0.20 cm in air is roughly equivalent to 1 micron in emulsion, and straggling (see below) and experimental uncertainties further limit the accuracy of determinations, this factor may be safely ignored in using Eqs. (2–7) to (2–11).

Experimental Relationship

The range-energy relationship for proton and alpha-particles has been experimentally determined in a number of investigations, the most comprehensive having been those of Lattes, Fowler, and Cüer (1947a, b) and Bradner *et al.* (1950). The former authors employed Ilford B1 emulsions and the latter C2 emulsions in their work; however, there seems to be no significant difference in the stopping powers of Ilford B1, B2, C2, C3, E1, and G5 and Kodak Ltd. NT2a emulsions (Bradner *et al.*, 1950; Rotblat, 1950). Since the range-energy curves included by Eastman Kodak with their technical data agree very closely with the above figures, and the compositions of the various emulsions are all about the same (Sec. 1–3), it may be concluded that these results apply quite well to most emulsions at present manufactured.

The measurements of Lattes *et al.*, made using particles produced in nuclear transmutations, are given in Table 2–I for protons and alpha-particles up to 13 Mev. The accuracy of these figures is ±2 percent above 2 Mev. Camerini and Lattes (1947) have provided the extrapolation of these results to 35 Mev with a believed accuracy of ±8 percent. The work of Bradner *et al.* on protons between 7.8 and 39.5 Mev obtained from the Berkeley cyclotron, Table 2–II, are in very close agreement with the extrapolation, indicating the probable reliability of the extrapolated values for alpha-particles. The proton measurements are accurate to at least 2 percent and probably better.

It is interesting to note the effect on the ranges of differences in atmospheric humidity; a range of 1497 microns was obtained for 17.6-Mev protons when the emulsions were maintained at about 80 percent relative humidity, and 4762 and 4996 microns for 33.5-Mev protons at 80 and 90 percent, respectively. This effect in due to the absorption of moisture by the gelatin of the emulsion (see below). Another result of these experiments was an approximate value for the range of 30-Mev protons in the glass backings of the plates. The range was found to be 18±4 percent greater in the glass than in the emulsion.

At high velocities, when plotted on logarithmic scales, the range-energy curves are very nearly straight lines (Fig. 2–6). Now integrating

$$dE/dx = z^2 f_1(v) = z^2 f_2(E/M), \tag{2–13}$$

we obtain

$$E = M f_3(z^2 R/M). \tag{2–14}$$

By making use of the linearity of the log R *vs* log E curves we obtain for f_3 the relation

$$f_3(z^2 R/M) = K(z^2 R/M)^n, \tag{2–15}$$

where K is constant and the exponent n constant over a relatively large region. In this region it is possible to calculate directly the range-energy relationship for particles of any mass and charge without using Eqs.

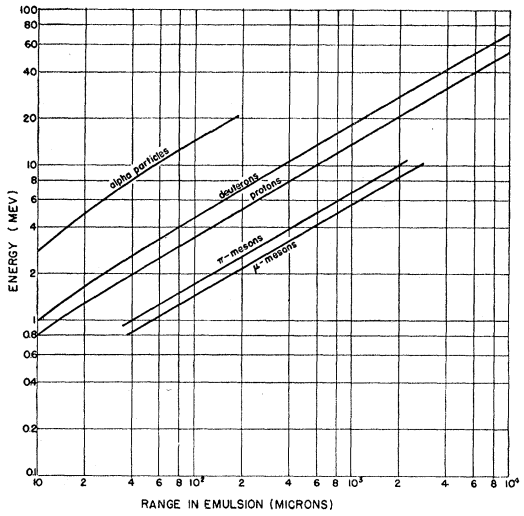

Fig. 2–6. Range-energy relationship in nuclear emulsions for various particles.

(2–7) and (2–10) since, from Eq. (2–14),

$$E = K z^{2n} M^{1-n} R^n. \tag{2–16}$$

Lattes *et al.* (1948) give $K = 0.262$ and $n = 0.575$ when M is given in terms of the proton mass, R in microns, and E in Mev. In Fig. 2–6 the meson curves were obtained by means of Eq. (2–16).

The evaluation of the range-energy relation for electrons is rendered very difficult because of the considerable scattering in their tracks. Ross and Zejac (1948), using an electron spectrograph, and Herz (1949), using an electron microscope and photoelectrons from x-rays, have determined this relation in Kodak NT2a emulsions. Their results are summarized in Fig. 2–7 and have been extrapolated to energies above the ~80-Kev maximum electron energy that can be recorded in NT2a emulsions. This curve may be expected to apply to other electron-sensitive plates considering the errors involved in electron range measurements.

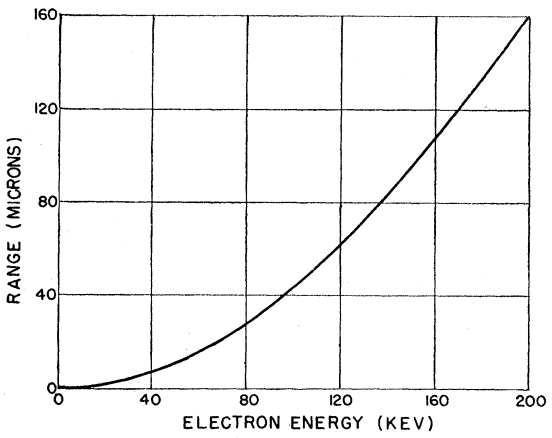

Fig. 2–7. Relationship between electron energy and range in emulsion (Herz, 1949).

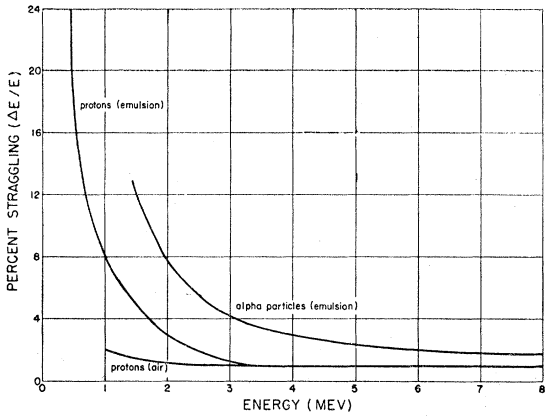

Fig. 2–8. Energy straggling of proton and alpha-particle tracks in emulsion (Rotblat, 1950) and of protons in air (Livingston and Bethe, 1937).

Straggling

In this discussion it has been assumed that the range of a particle of given energy is entirely constant and that any uncertainties present are the result of experimental errors. However, fluctuations in the ranges of mono-energetic particles will apparently occur because of the discontinuous nature of the ionization processes, and these fluctuations (straggling), while of the order of only one percent in air, become of greater importance in the emulsion due to the finite size and relatively small number of the grains making up a track. In addition, the halide grains of the emulsion are not homogeneously distributed in the gelatin, leading to regions of lower than average grain concentration and adding to the uncertainty in the precise value of the range. Rotblat (1950) defined the straggling γ as

$$\gamma=\left(\frac{\pi}{2}\right)^{\frac{1}{2}}\left[\frac{\sum_N(R_N-R_0)^2}{N}\right]^{\frac{1}{2}} \qquad (2\text{–}17)$$

for the ranges R_N of tracks produced by a homogeneous beam of particles, where R_0 is the average range and N the total number of tracks. Alternatively, the straggling may be given in terms of the half-width ΔR of the differential curve at half the maximum amplitude. For a Gaussian distribution ΔR is given by

$$\Delta R=2\gamma(\ln 2)^{\frac{1}{2}}/\pi^{\frac{1}{2}}=0.94\gamma. \qquad (2\text{–}18)$$

The straggling is usually expressed as $100\Delta R/R$, the percentage uncertainty in the range, or as $100\Delta E/E=100n\Delta R/R$, the uncertainty in the energy, where n is the range-energy exponent [Eq. (2–15)].

Powell *et al.* (1946), Lattes *et al.* (1947b), and Nereson and Reines (1950) have experimentally determined the straggling of various particles. The energy straggling of protons and alpha-particles between 0.4 and 8 Mev is shown in Fig. 2–8 (Rotblat, 1950) with the corresponding straggling for protons in air (Livingston and Bethe, 1937) provided for comparison.

TABLE 2-III. The ranges of protons of different energies in emulsions containing various amounts of water. The ranges are given in microns.

Energy Mev	Relative volume of water in emulsion 0.5	0.6	0.65	0.68	0.7	0.72	0.74	0.76
1	17.4	18.1	18.5	18.7	18.9	19.1	19.2	19.4
2	50.3	53	54.4	55.3	56	57	57	58
3	91.1	96	98	99.5	100	101	103	104
4	152	160	165	168	171	173	175	178
5	226	240	248	253	256	260	264	268
6	311	331	343	351	355	361	365	372
7	407	434	450	461	467	475	481	490
8	514	549	570	584	592	602	610	622
9	632	676	703	720	730	743	753	766
10	761	815	848	868	881	897	909	926
11	899	964	1003	1027	1043	1062	1076	1097
12	1046	1123	1168	1197	1216	1238	1256	1280
13	1204	1293	1346	1379	1402	1427	1448	1476
14	1379	1485	1542	1580	1606	1635	1660	1691

Wet Emulsions

When it is necessary to expose wet emulsions, as in the case of deuterium loaded plates (Sec. 5–5), or it is desired to correct exactly for humidity variations, the above quantitative relationships must be modified somewhat. Curves giving the specific energy loss of protons in Ilford emulsions, taken from the data of Lattes *et al.* (1947), and in water, as determined from range-energy curves for protons in oxygen and hydrogen (Aron *et al.*, 1949) tabulated by Krohn and Shrader (1951), are given in Fig. 2–9. Average rates of energy loss in a wet emulsion may be determined from these curves by adding the values for any energy multiplied by their relative volume in the emulsions. On the basis of this procedure Krohn and Shrader have calculated the ranges of protons of different energies in Ilford emulsions containing various amounts of water (Table 2–III). These values may be extended to cover particles of different masses by the equations discussed above. Range-energy values for wet emulsions can also be obtained by calculating their stopping powers by the method given below.

In order to correct for the swelling of the emulsion due to the absorbed water when determining track lengths a shrinkage factor S' must be evaluated. The range of a particle is then

$$R=[Y^2+(S'Z)^2]^{\frac{1}{2}}, \qquad (2\text{–}19)$$

where Y is the projected track length in the plane of the emulsion and Z the difference in depth between the ends of the track. S' is given by the emulsion thickness at the time of exposure divided by its thickness after processing, and may be obtained either by direct measurement or by calculation. In the latter case the equation

$$S'=(ST_0+T_w)/T_0 \qquad (2\text{–}20)$$

may be used, where S is the usual shrinkage factor (Sec. 3–6), T_0 is the emulsion thickness after processing,

TABLE 2-IV. Atomic stopping powers for various velocities and particle energies (Livingston and Bethe, 1937; Webb, 1948).

Velocity ($\times 10^9$ cm sec^{-1})	Energy: Alpha-particles (Mev)	Energy: Protons (Mev)	Stopping Power s: Ag	Br	C	H	N	O	Air
1.0	2.07	0.52	2.25	2.07	0.940	0.260	1.02	1.10	1.0
1.5	4.66	1.17	3.08	2.68	0.932	0.224	1.02	1.10	1.0
2.0	8.30	2.09	3.43	2.94	0.921	0.209	1.01	1.10	1.0
2.5	12.95	3.26	3.64	3.10	0.914	0.200	1.01	1.09	1.0
3.0	18.60	4.70	3.76	3.19	0.908	0.194	1.00	1.09	1.0
4.0	33.21	8.36	3.93	3.30	0.899	0.186	1.00	1.08	1.0
5.0	51.9	13.06	4.04	3.38	0.892	0.181	0.99	1.08	1.0

and T_w is the thickness of water added. In terms of the mass of water present on a 1-in. by 3-in. plate,

$$T_w = 0.517\ M_{H_2O} \text{ microns} \tag{2-21}$$

or

$$T_w = 0.465\ M_{D_2O} \text{ microns}, \tag{2-22}$$

where the masses of ordinary water and heavy water are expressed in milligrams (Krohn and Shrader, 1951). The water mass is found by weighing the emulsion both dry and wet. It is important to note that wet plates lose several milligrams of water per minute in air, although this rate may be diminished by the use of proper containers which can be maintained at a saturated atmosphere.

Stopping Power

The stopping powers of nuclear emulsions, defined as the ratios of the ranges of given particles in air at STP to their ranges in emulsion for specific energy intervals, are very useful quantities since they enable the immediate conversion of range-energy values in air to the corresponding values in emulsion.

It is usually possible to determine stopping powers experimentally; however, a theoretical expression enables stopping powers to be calculated for any reasonably homogeneous substance, and so can be used to predict, for example, values for wet emulsions and emulsions diluted with gelatin. The stopping power of an element of atomic number Z relative to air is given by

$$s = B/B_0, \tag{2-23}$$

where

$$B = Z \ln(2mv^2/I) \tag{2-24}$$

is a dimensionless quantity from the energy loss formula Eq. (2–1) for the stopping atoms and B_0 is the corresponding quantity for air. B, the "stopping number," has been evaluated by Livingston and Bethe (1937) for particle velocities from 1×10^9 to 5×10^9 cm sec^{-1} in a number of cases, and Webb (1948) has obtained by interpolation from these figures values for the atomic stopping powers of the emulsion constituents. These are given in Table 2–IV along with the alpha-particle and proton energies corresponding to these velocities.

In order to calculate stopping powers for emulsions from this information, a method given by Cüer (1946) and Webb (1948) must be used. The definition of s for a specific material means that

$$R_0/R = (N/N_0)s, \tag{2-25}$$

where R_0 is the range in air for a particle and R the range in the material, N_0 the effective number of atoms per cm^3 in air at STP based upon mean atomic weight, and N the number of stopping atoms per cm^3. Since what are actually being measured experimentally are the ratios $\Delta R_0/\Delta R$ of the differential ranges for small energy increments, the form

$$\Delta R_0/\Delta R = (N/N_0)s \tag{2-26}$$

will be used. Since

$$N = kd/A, \tag{2-27}$$

with d being the density of the substance and A the atomic weight of its constituent atoms,

$$\Delta R_0/\Delta R = n\textstyle\sum_i N_i s_i/N_0, \tag{2-28}$$

where N_i is the number of atoms of the ith kind in each molecule with a stopping power of s_i, and

$$n = d/\textstyle\sum_i N_i A_i \tag{2-29}$$

is the number of molecules per cm^3. Hence

$$\Delta R_0/\Delta R = (A_0 d/d_0)(\textstyle\sum_i n_i s_i/\sum_i N_i A_i), \tag{2-30}$$

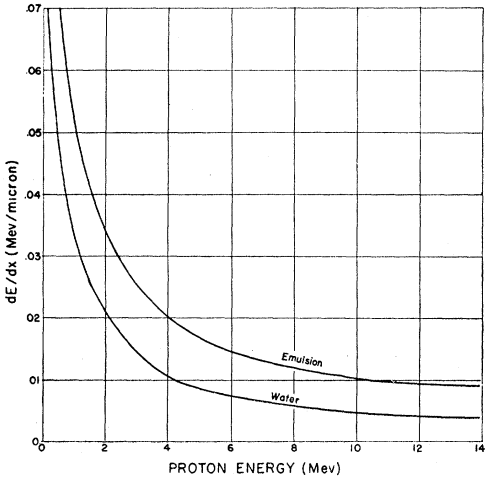

Fig. 2–9. The specific energy loss of protons as a function of energy in Ilford emulsions and in water.

or, in a form more easily adapted to calculation,

$$\Delta R_0/\Delta R=(A_0 d/d_0)\sum_i p_i s_i/A_i. \qquad (2\text{–}31)$$

The quantity

$$p_i=N_i A_i/\sum_j N_j A_j \qquad (2\text{–}32)$$

is the fractional weight of each element in the compound.

Although nuclear emulsions are actually suspensions of silver bromide crystals in a gelatin matrix, and so mixtures rather than compounds, Eq. (2–31) may be employed under the assumption that the resulting inhomogeneity is negligible when compared with the particle ranges. Inserting the values of the s_i from Table 2–IV in Eq. (2–31) for a specific emulsion enables the evaluation of $\Delta R_0/\Delta R$ at the various energies. To find the integral stopping powers R_0/R it is necessary to divide differential range values in air ΔR_0 over small energy intervals (one or two Mev) by the corresponding values of $\Delta R_0/\Delta R$ to obtain the equivalent differential ranges ΔR in emulsion. Summing these ΔR values then gives the integral emulsion ranges R. Dividing R_0, obtained by summing the ΔR_0 values, by R gives the integral stopping powers. Webb has given curves of R_0/R as a function of energy for an emulsion containing 82 percent silver bromide, which therefore might be expected to be similar to most commercial emulsions (Fig. 2–10). The experimental results of Lattes *et al.* (1947b) in the region below 13 Mev are in agreement with these curves.

2–4. TRACK IDENTIFICATION

By means of the above information tracks can be identified as to the mass and energy of the particles involved on the basis of range and grain count measurements. Track differentiation techniques, by accentuating the differences between the grain structures of tracks, are of great assistance with the methods to be described. However, with electron-sensitive emulsions when the full sensitivity is required, many tracks will be continuous and other means of identification must be employed. Either the optical densities of such tracks or the results of scattering measurements (Sec. 2–7) can provide mass estimates if necessary. Tracks due to particles of charges greater than two can be evaluated on the basis of delta-ray and taper length analyses (Secs. 2–5 and 2–6). Scattering along with ionization measurements can be used for Li, Be, and B nuclei.

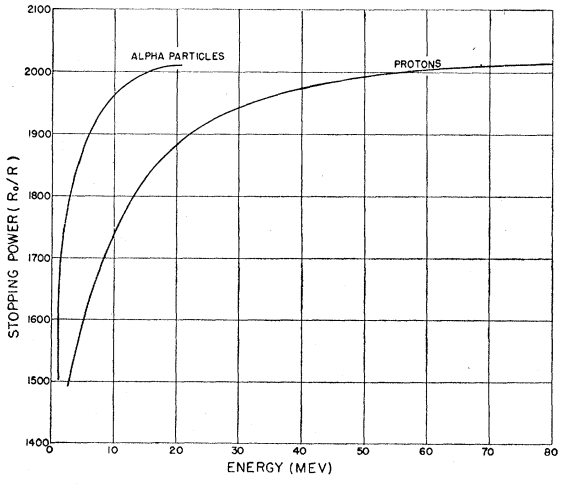

FIG. 2–10. Integral stopping powers of nuclear emulsions as a function of particle energy (Webb, 1948).

Tracks Ending in Emulsion

Mass determinations can be made easily on tracks ending in the emulsion by means of grain counts. For singly charged particles Eq. (2–14) gives

$$E=Mf(R/M). \qquad (2\text{–}33)$$

The total number of grains N in a track is certainly a function of the initial particle energy E, and so

$$N=MF(R/M), \qquad (2\text{–}34)$$

where F has the same form for all mass values. Hence, for two particles a and b,

$$N_a=M_a F(R_a/M_a) \qquad (2\text{–}35)$$

and

$$N_b=M_b F(R_b/M_b). \qquad (2\text{–}36)$$

If the values of $F(R/M)$ in Eq. (2–35) and (2–36) are equal, then

$$N_b/N_a=M_b/M_a=r \qquad (2\text{–}37)$$

and

$$R_b/R_a=M_b/M_a=r, \qquad (2\text{–}38)$$

where r is the ratio of the two masses. Therefore,

$$\log N_b-\log N_a=\log r, \qquad (2\text{–}39)$$

and, simultaneously,

$$\log R_b-\log R_a=\log r. \qquad (2\text{–}40)$$

On a logarithmic plot of N *versus* R, such as the one in Fig. 2–11 taken from the data of Lattes *et al.* (1947c), these relations imply that points of equal $F(R/M)$ on the various curves may be found by drawing 45° lines between them. A value for r then follows immediately. If a particular emulsion has been calibrated in this way, singly charged particles can be identified on the basis of plots such as those in Fig. 2–11.

Since the curves for the various particles are linear over most of their ranges,

$$F(R/M)=K'(R/M)^{n'} \qquad (2\text{–}41)$$

and so

$$N=K'M^{1-n'}R^{n'} \qquad (2\text{–}42)$$

as in the case of the range-energy relationship. M is expressed here in units of the proton mass and, for Ilford C2 boron loaded emulsions, $K'=76$ and $n'=0.711$

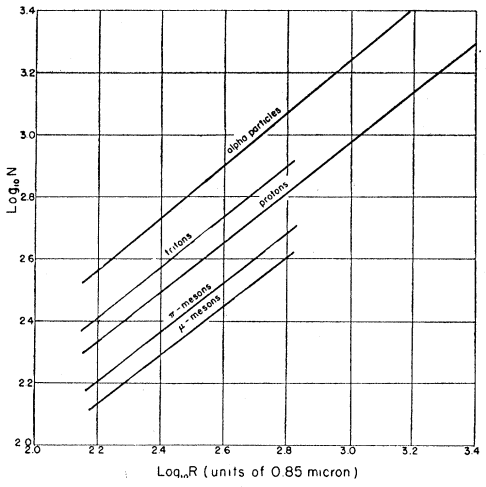

FIG. 2–11. The variation of the total number of grains N with residual range R for tracks of various particles in Ilford C2 boron-loaded emulsions (from data of Lattes *et al.*, 1947c).

(Lattes *et al.*, 1948). For particles of z greater than 1,

$$N = K' z^{2n'} M^{1-n'} R^{n'}. \tag{2–43}$$

Another method of mass evaluation employs the relationship between the grain density dN/dR at any point and the distance R of that point to the end of the track,

$$dN/dR = f'(R/M). \tag{2–44}$$

Thus, at points of equal grain density in the tracks of particles of masses M_a and M_b,

$$M_b/M_a = R_b/R_a. \tag{2–45}$$

Inaccuracies in the use of these techniques can arise when the tracks being compared are of different age and fading has occurred. In addition, in the case of thick emulsions, the extent of development may vary somewhat with depth despite precautions to minimize this effect. However, under favorable conditions comparative mass measurements of a good degree of precision are possible. For example, these techniques were first employed in the evaluation of meson mass ratios where, since the tracks were formed at the same time and in the same region of the emulsion, reliable values could be obtained.

Track Segments

If a track does not terminate within the emulsion, the variation in its grain density, when sufficiently great, can provide an estimate of the mass of the particle that produced it. In Fig. 2–12 are plotted curves showing the relationship between the residual ranges in emulsion of various particles and their specific energy losses in Mev/(g/cm²) (Bradt *et al.*, 1950). Each emulsion used must be calibrated to give the appropriate conversion between grain density and specific energy loss. To convert the experimental curves obtained, such as that given in Fig. 2–2, to energy losses in Mev/(g/cm²) the relation

$$10^4 \text{ microns of emulsion} \doteq 4.0 \text{ g/cm}^2 \tag{2–46}$$

must be used.

To identify a given track segment, if we assume a particle with unit charge, the grain densities at two points as far apart as possible are determined. The smaller density, corresponding to the higher energy of the particle at that point, is then used in conjunction with Fig. 2–12 to give the expected residual ranges of the various possible particles for that rate of energy loss. The specific energy losses to be expected of these particles after traversing the two experimental points may be found by following the various curves down the appropriate distance on the ordinate of the graph. The energy loss value thus obtained corresponding to the higher observed grain density then provides the identity of the particle. The energy of the particle is then obtained from range-energy curves (Fig. 2–6) by use of the value of the expected residual range.

Figure 2–12 can also be used with tracks ending in the emulsion. The grain density of the track at its point of entry into the emulsion, expressed in terms of energy loss, and the residual range are merely compared with these curves to identify the particle causing the track.

Slide Rule

The approximate linearity of the range-energy, range-grain density, and residual range-total grain count curves when plotted logarithmically was made use of by Beiser (1950c) in the construction of a simple slide rule to facilitate track evaluation. The scales of the rule are most conveniently laid out as in Fig. 2–13, being calibrated from the experimental curves for each

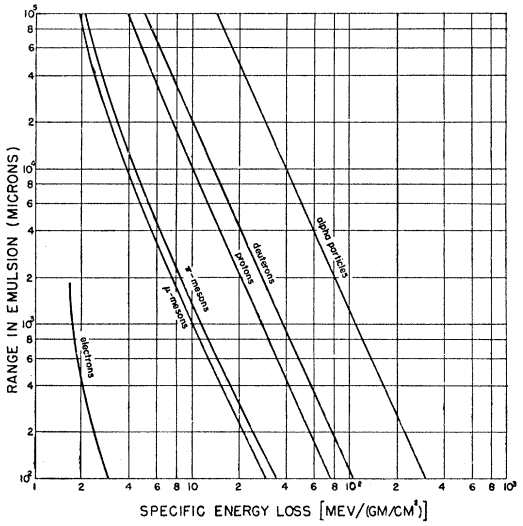

FIG. 2–12. The specific energy loss of various particles in nuclear emulsions as a function of their residual ranges, where 10^4 microns of emulsion $\cong$4.0 g/cm² (Bradt *et al.*, 1950).

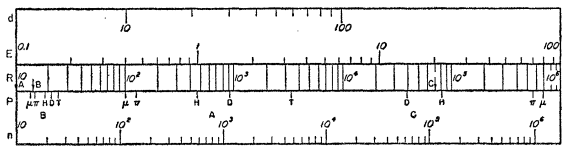

FIG. 2–13. Arrangement of scales for track evaluation slide rule (Beiser, 1950c)

combination of emulsion and processing. The range (R), energy (E), grain density (d), and grain count (n) scales are taken directly from the appropriate curves. The P scale, giving the particle identity, is determined by selecting an arbitrary value of R, finding the corresponding value of E, d, or n for the various particles, and setting them opposite the R value. The identity of the particles then appears opposite the appropriate arrow on the R scale. The A arrow is used for R *vs* E, the B arrow for R *vs* n, and the C arrow for R *vs* d.

In using the slide rule the particle identity is first determined in the same way as with the curves. If the track ends in the emulsion, the grain count n in a distance R in microns from the end may be set against this value of R, and the nature of the particle will then be adjacent to arrow B. As a check, or if the track does not end in the emulsion, the grain density d in grains per 100 microns at two points on the track as far apart as possible should be measured. The arrow C may then be set against the various particles on P, and their ranges corresponding to the smaller grain density read off on R. The distance between the two experimental points is then subtracted from the range values thus obtained, and the arrow C reset against the new ranges. The grain density corresponding to the greater of the measured ones then gives the identity of the particle.

The energy of a particle ending in the emulsion may be found from the R and E scales using the arrow A. For identified track segments the range corresponding to the smaller grain density can be used to find E.

2–5. DELTA-RAYS

Particles of charge greater than two produce tracks with virtually no grain structure even at high energies, the tracks appearing as solid filaments of silver (Fig. 2–14). Such energetic heavy ions are to be found principally as components of the cosmic radiation at high altitudes (Freier *et al.*, 1948a). The rates of energy loss of these particles are so great that secondary electrons are produced with sufficient energies to have observable ranges in an emulsion. The number of such electrons or delta-rays is a function of dE/dx and, in conjunction with range determinations, provides a means of estimating the charges and energies of these particles.

Theoretical Number

Following Bradt and Peters (1948), a theoretical expression for the number n of delta-rays per centimeter will be obtained. The number dn of such rays with energies between W and $W+dW$ has been given by Mott (1929) as

$$dn=\frac{2\pi Nz^2e^4}{mv^2}\frac{dW}{W^2}\left[1-\frac{(1-\beta^2)}{2}\frac{W}{mc^2}+\frac{z\pi\beta}{137}\left(\frac{1-\beta^2}{2\beta^2}\frac{W}{mc^2}\right)^{\frac{1}{2}}\left(1-\frac{1-\beta^2}{2\beta^2}\frac{W}{mc^2}\right)\right], \quad (2\text{–}47)$$

where m is the electron mass, z and v the charge and velocity of the incident particle, and N the density of electrons in the stopping material. The cross section for elastic scattering of electrons by the Coulomb field of a nucleus of charge z has been transcribed in this equation to the coordinate system in which the electron is intitially at rest. As in the relationship for dE/dx, the mass of the particle does not appear.

It is possible to identify delta-rays only if they are properly oriented for observation and have energies within a certain interval. The upper energy limit W_2 depends upon the sensitivity of the emulsion to electrons (see Sec. 1–3 for specific values for various commercial emulsions) and the lower one W_1 upon the criterion employed to distinguish short delta-ray tracks from random background grains. Freier *et al.* (1948b) take the minimum acceptable track length to be 1.5 microns, while Bradt and Peters use four grains in a

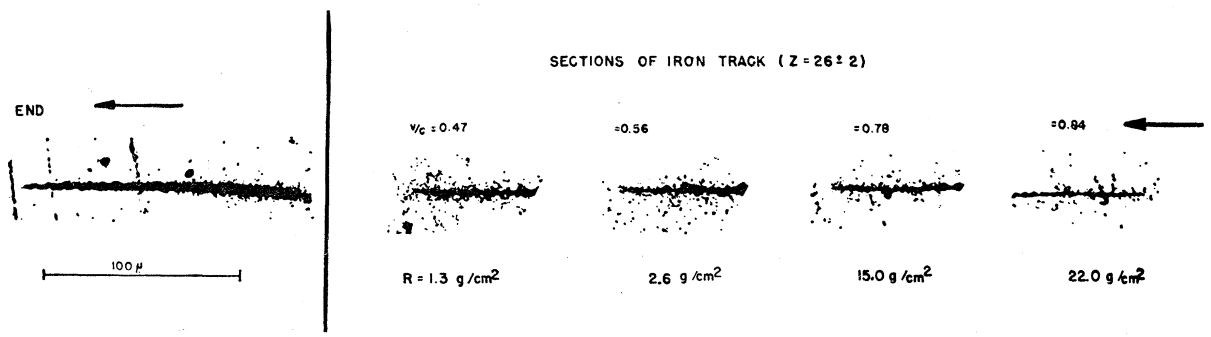

FIG. 2–14. Sections of the track left by a 62-Bev iron nucleus in a stack of nuclear emulsions exposed to cosmic radiation at a high altitude (Bradt and Peters, 1949).

row as their minimum. Both procedures give a lower limit in the vicinity of 10 kev.

The maximum delta-ray energy for a given β is $2mc^2\beta^2$ in the nonrelativistic approximation, m again being the electron mass. The lowest value of β which will result in the production of delta-rays with maximum energies W_2 is therefore determined by the condition that

$$\beta \geqslant W_2/2mc^2. \tag{2-48}$$

For $W_2=30$ kev, corresponding to the maximum electron energy that can be recorded in Ilford C2 emulsions, this implies that Eq. (2-47) is applicable for residual ranges in the emulsion of greater than 1200 microns for alpha-particles. For completely ionized carbon atoms the minimum residual range is about 400 microns, and lower values apply for still heavier atoms. Hence, Eq. (2-47) is valid for most heavy particle tracks until comparatively short distances from their ends.

For delta-rays of energies between 10 and 30 kev the bracketed relativistic correction term results in corrections of less than eight percent for values of z up to $z=30$. Thus it is possible to neglect this term without introducing any greater error than that already present in the experimental techniques. Integrating the remaining part of Eq. (2-47) then gives for n, the number of delta-rays of energies in the interval between W_1 and W_2,

$$n=\frac{2\pi Nz^2}{\beta^2}\left(\frac{e^2}{mc^2}\right)^2\left(\frac{mc^2}{W_1}-\frac{mc^2}{W_2}\right). \tag{2-49}$$

Regardless of the criteria employed in identifying delta-rays, a constant fraction of this theoretical number should be obtained. Bradt and Peters give 16 percent as the value of this fraction for delta-ray counts made on 168-Mev and 368-Mev cyclotron alpha-particles recorded in Eastman NTB emulsions, and 10 percent for cosmic-ray alpha-particles of about 60 Mev in in Ilford C2 emulsions.

According to Eq. (2-49) n should vary as z^2/β^2. The $1/\beta^2$ dependence is actually not quite correct, however, as is evident from Fig. 2-15 (Freier *et al.*, 1949b). These curves give the number of delta-rays with energies greater than W_1 for values of W_1 between 5 and 50 kev as a function of β relative to the corresponding values of n for $\beta=1$, i.e., $v=c$. If n varied as $1/\beta^2$, at $\beta=0.35$ the ordinates of these curves should all be $1/(0.35)^2$ or 8.2, which is only approximately true. However, for $W_1\leqslant 10$ kev the deviation from a $1/\beta^2$ dependence is insignificant for most purposes.

Experimental Application

In order to determine the charge of the particle responsible for a track exhibiting a certain n at a residual range R, it is necessary to know the precise variation of n with R for various values of z. Now

$$n/n_\alpha=z^2\beta_\alpha^2/z_\alpha^2\beta^2, \tag{2-50}$$

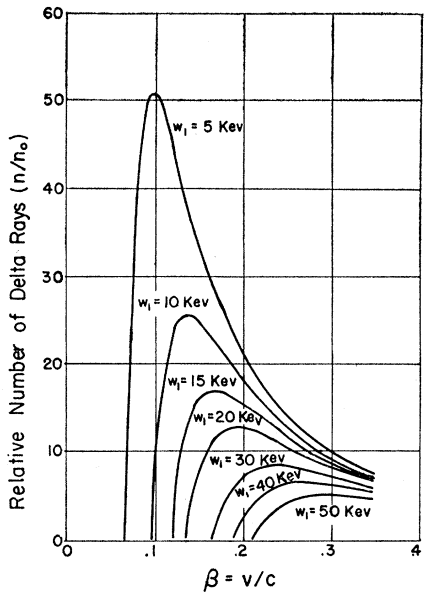

FIG. 2-15. Number of delta-rays of energy greater than W_1 relative to the corresponding number when $v=c$ as a function of β (Freier *et al.*, 1949b).

where n_α is the delta-ray density of an alpha-particle track at a point corresponding to a residual range R_α and a velocity $\beta_\alpha C$, and β^2 is a known function of $Rz^2/M\approx Rz/2$, $M\approx 2z$ being the particle mass, given by

$$\beta^2=\psi(Rz/2). \tag{2-51}$$

The equation

$$n=\frac{z^2}{4}\frac{n_\alpha\psi(R_\alpha)}{\psi(Rz/2)} \tag{2-52}$$

then follows immediately. Bradt and Peters have plotted log n *versus* log R for various values of z as calculated from Eq. (2-52) in Fig. 2-16.

For a track that ends in the emulsion it is possible to find z very accurately, since n may be measured at various values of R and, using curves such as those in Fig. 2-16, several independent determinations may be performed for the same track. When the particle does not stop in the emulsion a value of z may be estimated by considering the variation of n along the track. If n remains relatively constant for several g cm^{-2} of track length, upper and lower limits for z may be obtained from n *versus* R curves.

When n varies significantly, it is necessary to guess a value for z and then, by trial and error, successively approximate the actual value. Alternatively, a less involved method for finding an approximate value of z consists of assuming for the upper limit to z that the track was of minimum ionization for its charge at the point of entrance into the emulsion, and for the lower limit that the known range in the plate or plates it is observed in corresponds to its actual range.

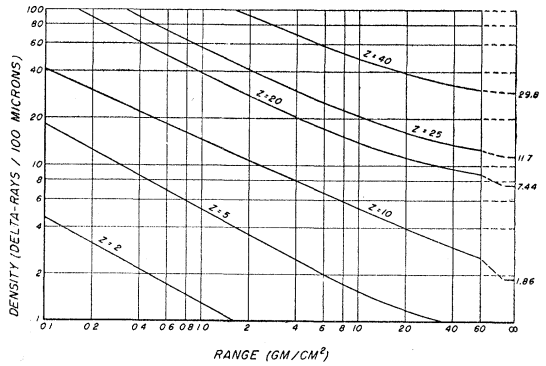

FIG. 2–16. Variation of delta-ray density with range in emulsion for various values of Z (Bradt and Peters, 1948).

2–6. TAPER LENGTH

An ingenious method for estimating the atomic number of multiply charged incident particles can be employed if their tracks terminate in the emulsion (Freier *et al.*, 1948). Such tracks increase in width along their trajectories until a point near the ends where they become narrower and ultimately stop. An example of this thinning down or tapering of heavy nucleus tracks is given in Fig. 2–14 which shows various segments of the track left by an iron nucleus with an original energy of 62 Bev in a stack of nuclear emulsions (Bradt and Peters, 1949). The tapering occurs because the initially stripped nuclei capture electrons when their energies have become sufficiently small, reducing their effective charges and hence their rates of energy loss. The length of the tapered portion of a track may be used to calculate an approximate value for the atomic number z of the particle involved if it is assumed that electron capture first occurs when its velocity is equal to that of the electrons which should occupy its K shell. Since the K electron velocities are proportional to z, the taper length L should therefore be a function of z as well. Assuming that the nuclear mass is $2z$ times that of the proton, its first electron will be acquired at an energy of $0.05z^3$ Mev. Taking its energy E to be $0.05zz'^2$ Mev at all energies below this, z' being the effective charge of the particle at each such energy, L may be found by numerically integrating

$$L=\int_0^z (dx/dz)dz=\int_0^z (dE/dz)/(dE/dx)dz. \quad (2\text{–}53)$$

The value of dE/dz is obtainable from that of dE/dx and from the above relationship between E and z by multiplying the energy loss curves for protons of the same velocity (Sec. 2–2) by z'^2. Alternatively dE/dx for protons may be found by differentiating the appropriate range-energy curve (Sec. 2–3). In Fig. 2–17 the relationship between the atomic numbers of incident nuclei and their taper lengths has been plotted from these considerations (Freier *et al.*, 1948). In contrast to these results, which give $L\approx 0.5z^2$, Hoang and Morellet (1950) find experimentally that an equation of the form $L=az^\alpha$ provides a better fit with their data, where α is approximately unity. Further work is necessary to clarify this point.

2–7. MULTIPLE SCATTERING

A charged particle moving through matter undergoes frequent small deflections due to elastic collisions with the atomic nuclei in its path. Bose and Choudhuri (1941), making use of the dependence of the degree of scattering upon the mass and energy of the particle involved, suggested the use of scattering measurements in the determination of these quantities. Subsequent work by Perkins (1947), Occhialini and Powell (1947), and others mentioned below has indicated the usefulness of techniques based upon the evaluation of such scattering.

Theory

The earliest theoretical treatment of the scattering problem in a form suitable for comparison with experiment was given by Williams (1939, 1940). He evaluated the mean angular deflections α due to all scattering experienced by a particle of charge z, momentum p, and velocity v in traversing a distance x in a medium of N atoms of atomic number Z per cm³, and found a Gaussian distribution of α about $\alpha=0$. The probability for the occurrence of an individual deflection ϕ follows Rutherford's scattering law. Both α and ϕ are the projections on a plane of the space angles of the scatterings, and so are in a convenient form for plate measurements. The mean value of ϕ was given by Williams as

$$\langle\phi\rangle=\frac{2ze^2(Z^2Nx)^{\frac{1}{2}}}{pv}[\ln(\phi_{\max}/\phi_{\min})]^{\frac{1}{2}}, \quad (2\text{–}54)$$

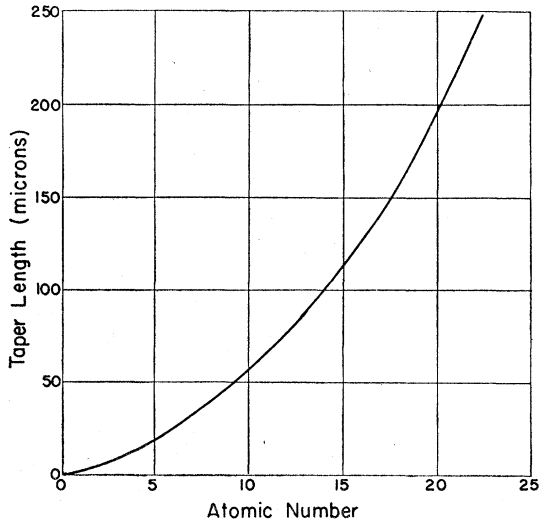

FIG. 2–17 Theoretical relationship between taper length and atomic number for heavy nuclei (Freier *et al.*, 1948).

where ϕ_{max} is the largest and ϕ_{min} the smallest deflection angle that can contribute to the observed scattering. It is convenient in discussing multiple scattering to define a unit angle δ as

$$\delta=\frac{2ze^2(Z^2Nx)^{\frac{1}{2}}}{pv}. \tag{2-55}$$

An approximate value for ϕ_{max} may be found by determining the angle ϕ_1 such that, in covering the distance x, the particle undergoes on the average one collision of $\phi>\phi_1$. This gives

$$\phi_{max}\cong\phi_1=(\pi/2)^{\frac{1}{2}}\delta. \tag{2-56}$$

Williams finds that, taking into account the screening due to the electron shells of the stopping atoms,

$$\phi_{min}=mcZ^{\frac{1}{3}}/78.3p, \tag{2-57}$$

in which m is the electron mass.

Equation (2-54) may be written in the form

$$\langle\phi\rangle=L\delta. \tag{2-58}$$

Other derivations, such as those of Molière (1947, 1948) and Snyder and Scott (1949), give somewhat different expressions for L. In general, however, $\langle\phi\rangle$ can be given as

$$\langle\phi\rangle=Kzx^{\frac{1}{2}}/pv, \tag{2-59}$$

where K, defined as the scattering constant, is

$$K=2e^2(Z^2N)^{\frac{1}{2}}L. \tag{2-60}$$

Although K depends primarily upon the characteristics of the scattering medium and so remains relatively constant for a given emulsion, it is interesting to evaluate its variation with the particle velocity βc and path length x. This has been done by Molière by making use of the quantity $\Omega_b=\pi\delta^2/\phi^2_{min}$, which is a measure of the mean number of collisions experienced by the particle in the distance x. Gottstein *et al.* (1951) have plotted Ω_b/x, where x is in units of 100 microns, as a function of β^2 for Ilford G5 emulsions for particles of unit charge (Fig. 2–18). The variation of K with Ω_b is shown in Fig. 2–19 for two cases, (a) the theoretical result and (b) the case in which all scattering angles greater than four times the mean are excluded. The values of K from curve (b) are approximately 10 percent smaller than those from curve (a). These curves have been experimentally verified by Gottstein *et al.*

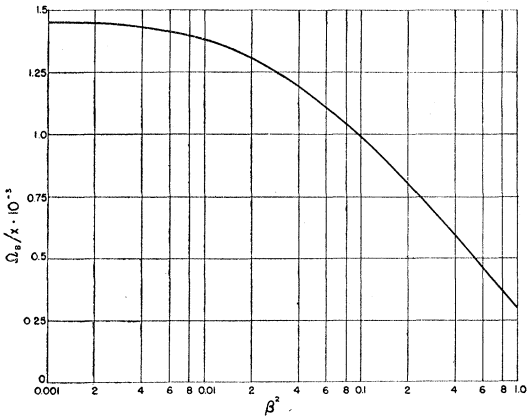

FIG. 2–18. The value of Ω_b/x as a function of β^2 for singly charged particles in Ilford G5 emulsions (Gottstein *et al.*, 1951).

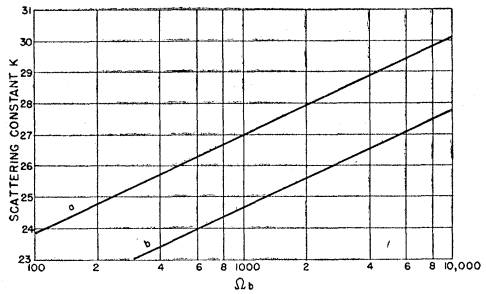

FIG. 2–19. The variation of the scattering constant K with the parameter Ω_b for (a) all scattering angles ϕ, and (b) only those angles less than four times the mean angle $\langle\phi\rangle$ (Gottstein *et al.*, 1951).

Experimental Technique

There are several methods in common use at present for measuring the multiple scattering of tracks in nuclear emulsions. In one, the tracks are divided into equal sections (cells), usually $x=100$ microns long, and the angles ϕ_t between tangents to the tracks in successive cells determined directly (Goldschmidt-Clermont *et al.*, 1948, Davies *et al.*, 1949; Goldschmidt-Clermont, 1950). Actually, of course, what is being measured are the angles between lines fitted visually to the track in each cell. A variant of this technique was employed by Lattimore (1948) in his work. Recognizing the difficulty of drawing visual tangents, he uses the angles ϕ_c between successive chords along the track to reduce the experimental error. The relationship between ϕ_c and ϕ_t is approximately

$$\phi_c=0.816\phi_t. \tag{2-61}$$

Another procedure was devised by Fowler (1950). In this method the track coordinates at cell intervals are measured and used to determine the mean values of ϕ_c between successive chords. Goudsmit and Scott (1948, 1949) have suggested using the difference between the actual length of a track interval and that of a straight line connecting the ends of the interval, i.e., the difference between track and chord lengths, to find the scattering angle.

Theoretically, for the case in which $\beta^2\cong1$, $K=24.45$ for 100-micron cells with ϕ given in degrees and pv in Mev. The experimental results of Gottstein *et al.* in a number of determinations are given in Table 2–V. K_a is the scattering constant as determined without imposing the restriction that each angle considered be less than four times the mean and K_b the constant with

TABLE 2-V. Experimental values for K_a, the scattering constant with no restrictions on ϕ, and K_b, the scattering constant with a cutoff for $\phi > 4\langle\phi\rangle$ (Gottstein *et al.*, 1951).

Particle	Energy	K_a	K_b
Positrons	105 Mev	26.7±0.6	26.2±0.6
Positrons	185 Mev	24.9±0.8	24.0±0.8
Protons	336 Mev	30.7±1.0	29.2±1.0
Protons and mesons	5–50 Mev	...	26.1±0.7
Protons	9–35 Mev	...	27.5±0.5

this restriction. The results of this investigation seem to indicate that, for ordinary work, taking $K = 26.0$ will not introduce an error of greater than 8 percent from this source, which is less than the usual experimental uncertainty in the angular measurements.

For the tracks of charged particles Eq. (2–59), together with the experimental value of $\langle\phi\rangle$, gives the particle energy E. If the track ends in the emulsion with a residual range R a comparison of these values of E and R with the range-energy curves for various particles (Sec. 2–3) will immediately give the particle mass. For track segments the variation $\langle\phi\rangle$ along the track can be used in conjunction with the range-energy curves to estimate the particle mass by a method similar to that given in Sec. 2–4. The values of $\langle\phi\rangle$ at a known distance apart in the track give the energies at those points; again comparison with range-energy curves provides a unique mass corresponding to this energy variation. Relative mass measurements are easily made from values of $\langle\phi\rangle$ obtained from track sections of equal grain density, since the particle velocities are equal at such points. Thus the ratio of the scattering angles is equal to the reciprocal of the ratio of the masses.

Errors in scattering determinations can arise in a number of ways, both personal and instrumental. As might be expected, spurious scattering (noise) increases with decreasing cell length. Gottstein *et al.* have investigated the noise obtained with a number of microscopes for different cell lengths. For $x = 50$ microns, the mean scattering angle due to noise was about 0.13°, for $x = 100$ microns about 0.09°, and for $x = 200$ microns about 0.055° with two different microscopes. A third microscope exhibited less noise, 0.035° at $x = 200$ microns, but the same rate of increase with smaller x values was observed. These spurious scattering angles must be determined in precision work for each instrument individually at the cell lengths employed, using straight tracks of high energy particles, and then subtracted from the measured angles found in tracks being evaluated.

Chapter 3. Emulsion Processing

3–1. GENERAL CONSIDERATIONS

For the purpose of processing, emulsions may conveniently be divided into two categories: those of less than 100-micron thickness, and those of this thickness and greater. The former are generally termed "thin" emulsions, and the latter "thick" emulsions. There are few difficulties to be encountered in the processing of thin emulsions, which proceeds almost exactly as in the case of ordinary photographic films and plates, while with thick emulsions the time required for the various solutions to penetrate fully necessitates the employment of more elaborate techniques.

Thin Emulsion Development

There are two degrees of development possible for thin emulsions, "moderate" and "strong." Moderate development is most useful when grain densities of comparatively dense tracks (such as protons and alpha-particles of several Mev energy) are to be measured. For such determinations it is essential that the grains be discrete rather than touching each other in order to remove ambiguity, and moderate development facilitates this. A further advantage is the great reduction in fog density that results from this treatment. However, the maximum sensitivity of the emulsion is not brought out, and the more weakly ionizing particle tracks may not be recorded. Strong development, on the other hand, permits full utilization of the emulsion sensitivity, although accompanied by an increased fog background. The tracks of heavily ionizing particles appear as solid columns of silver grains, rendering grain counts on them impossible. The best procedure in general is to conduct a series of development tests to determine the development time that gives the most preferable combination of background and track densities for the determination to be made.

In Table 3–I are the processing instructions recommended by Eastman Kodak for their thin emulsions, which may also be used for emulsions of similar dimensions of other manufacture. The formula for D19 is given in Table 3–II. In this formula the elon and hydroquinone are the actual developing agents, the other constituents being required for various specific purposes. The sodium carbonate is employed to adjust

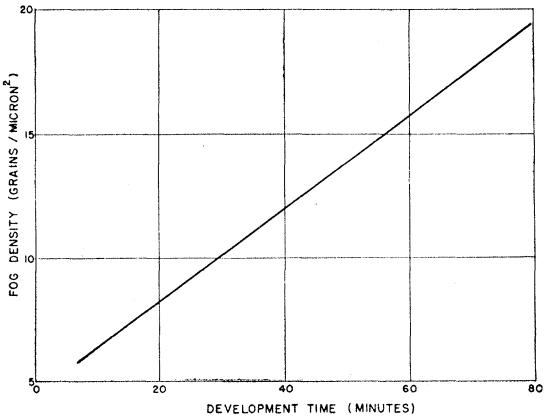

FIG. 3–1. Variation of mean fog grain density with developing time (Coates, 1951).

TABLE 3-I. Processing procedure for 10-, 25-, and 50-micron emulsions recommended by Eastman Kodak. Development is with undiluted D19, and all steps are to be carried out at 20°C.

Procedure	Time
10 microns, moderate development	2–4 minutes
25–50 microns, moderate development	4 minutes
25–50 microns, strong development	20 minutes, no agitation 10 minutes, vigorous air agitation
Rinse (running water)	10 minutes
Fixation (Kodak fixing bath F5)	Twice time to clear
Wash (running water)	1 hour

the *p*H of the solution so as to increase the rate of development, and is frequently called the accelerator for that reason. Other alkalis, such as sodium hydroxide, borax, and sodium metaborate (Kodalk), are sometimes substituted for the carbonate. Another function of the accelerator is to soften the gelatin of the emulsion, rendering it more easily permeable.

Since the presence of the oxidation products of the developing agents has an adverse effect on the development process, a preservative must be added to remove them at the time of their formation. This is the function of the sodium sulfite.

The fourth component in virtually all developers is potassium bromide, which serves to restrain the reducing action of the developing agent on those halide grains that have not been irradiated. The effect of the bromide on the reduction of the "exposed" grains is much smaller, however, leading to preferential development of the latter. The inclusion of potassium bromide thus diminishes considerably the rate of formation of a fog background, although necessitating a somewhat longer development time. Prolonged development might thus be expected to increase the fog background; this is borne out in the work of Coates (1951), summarized in Fig. 3–1, which shows the increase in fog grain density with time of development. These results were obtained under special circumstances and, while illustrative of the rate of increase in fog to be expected, are not quantitatively applicable to the development procedures to be given here.

Safelights

These emulsions are not overly sensitive to light and so may be processed under safelight illumination. An orange-red safelight filter such as the Wratten No. 2 or Ilford "*S*" No. 902 may be employed for all emulsions with the exception of the Eastman NTA type, where a yellow filter, Wratten OA, is recommended. The plates should remain under a safelight until the completion of the fixation stage, when normal lighting may be used.

Stop Bath

Upon the completion of the development stage the developer action must be immediately arrested. With very thin emulsions immersion in running water alone is sufficient to accomplish this. For emulsions 25 or 50 microns in thickness and greater, however, the usual method is to reduce the *p*H of the plates below that value required for development by means of dilute ($\frac{1}{2}$–1 percent) acetic acid. Another approach frequently used in conjuction with the latter in the temperature development process is rapid cooling. Since development is a chemical process and so its velocity a function of temperature, such cooling provides rapid stopping action. Temperatures of the order of 5°C are usual with this technique.

TABLE 3-II. Developer formulas.

Amidol (*p*H 7.2)		Eastman D19b (*p*H 10.0)		Azol (*p*H 11.5)		Ilford ID19		Amidol-bisulfite (*p*H 6.7)	
(a)									
Amidol	3 grams	Metol	2.2 grams	Johnson's Azol solution	16 ml	Metol	4.5 grams	Amidol	3.0 grams
Sodium sulfite (anhyd.)	12 grams	Sodium sulfite (anhyd.)	72 grams	Potassium bromide (1%)	88 ml	Sodium sulfite (cryst.)	288 grams	Sodium sulfite (anhyd.)	6.7 grams
Distilled water	1 liter	Potassium bromide	8.8 grams	Distilled water	384 ml	Hydro-quinone	17.5 grams	Sodium bisulfite liquor[a] (Sp. Grav. 1.34)	1.4 ml
(b)		Distilled water to make	2 liters			Sodium carbonate (cryst.)	260 grams		
Amidol	4.5 grams							Distilled water	930 ml
Sodium sulfite (anhyd.)	18 grams					Potassium bromide	8 grams		
Potassium bromide (10% sol.)	8 ml					Distilled water to make	2 liters		
Distilled water	1 liter								

[a] This is a preparation obtainable from British Drug Houses Ltd.

Surface Deposit

As a result of the high concentration of silver bromide in nuclear emulsions and its partial solubility in the developer, a thin film of silver is usually formed on the surface of the emulsions during their development. This film may be so dense as to render scanning virtually impossible, and in any case impedes the careful examination of the plates. Removal of such a deposit may be done in the stop bath, by use of a wet chamois or, preferably, the finger tips. The emulsion is usually in a weakened condition at this point and care must be taken to prevent distortion. Alternatively, after processing and when the emulsion is completely dry, cotton or chamois moistened with alcohol may be used to wipe the silver off. At this time, however, the film is quite resistant and frequently it is difficult to remove it entirely. Stiller (1951) has had success with wiping the plates while they were being soaked in distilled water prior to development. A reduction in the amount of surface deposit may be accomplished (Dilworth *et al.*, 1950) by development in an inert atmosphere, or by using a developer such as azol (see Table 3–II) which usually leaves little or no deposit.

Fixation

The basic fixing bath for emulsion processing consists of a 30 to 40 percent solution by weight of sodium thiosulfate (hypo) in distilled water. Ammonium thiosulfate also acts as a fixing agent, but tends to remove developed grains near the emulsion surface. This objection also applies somewhat to the use of ammonium chloride for reducing the fixing time, although Stiller *et al.* (1951) employ it in a 0.7 percent concentration in their formula. Sodium bisulfite, which tends to reduce staining, has been used for this purpose in fixing baths in concentrations of from 0.75 percent by weight (Stiller *et al.*, 1951) to 3 percent (Dainton *et al.*, 1951).

Sufficiently large volumes of solution must be used or the bath renewed from time to time, as a consequence of the large amount of soluble silver salts to be removed. The fixing time varies considerably with such factors as the emulsion thickness, temperature, and extent of agitation employed, being for instance roughly proportional to the square of the thickness. A 400-micron emulsion may take 18 hours to clear, while for 1000 microns this time is more of the order of 100 hours. The best rule is to keep the plates in the fixing bath for a period 50 percent longer than the clearing time. Higher temperatures, up to perhaps 25°C, increase the speed of the process, although at the same time the danger of reticulation (see below) is greater. It is usually advisable with thick emulsions to reduce the hypo concentration gradually before washing by progressively diluting the solution in order to minimize distortion.

Agitation

The agitation of processing solutions is a common practice in ordinary photographic technique where it reduces significantly the periods of time involved. In the stop and fixing baths employed in processing nuclear emulsions agitation effects a similar reduction (Powell and Occhialini, 1947) with no deleterious results having been observed. However, agitation is not desirable in the development stage, especially with thick emulsions, since this would contribute to the differential in development rates between the emulsion interior and its surface by causing a more rapid exchange of exhausted developer with the fresh solution at the latter. In addition, violent agitation would increase oxidation of the developer and possibly also the surface deposit of silver on the plates, as well as adding significantly to distortion.

There are two types of agitation in general use, mechanical and gaseous. In mechanical agitation the solution may either be stirred with a small motor-driven propeller or the vessel containing the plates and solution rocked back and forth. When the plates are in a horizontal position, recommended for emulsion thicknesses greater than about 100 microns, the latter procedure produces an even laminar flow which is very effective (Powell and Occhialini, 1947). Stirring is usually easier to perform, but should not be violent enough to cause turbulence. The other method, in which a relatively inert gas, usually nitrogen, is bubbled through the bath, was investigated by Wilson and Vanselow (1949). The use of ordinary air in this procedure is not advisable, since the developed silver grains on the emulsion surface will then be oxidized. The nitrogen may be passed through an ordinary Büchner funnel, as in the experiments of Wilson and Vanselow, in order to provide a stream of small bubbles. Eastman Kodak recommends the use of a sintered glass filter for this purpose. When the solution is at other than room temperatures, a jacketed funnel permits passing water at the desired temperature around the gas before it enters the solution. A reduction of as great as 50 percent in fixing time is possible with gas agitation. It is, of course, unnecessary to know the precise value of the reduction obtained with any particular arragnement, the period to be spent in the fixing bath being one and a half times that required for the emulsion to clear.

Washing

The washing of the emulsion after fixation usually requires a period about equal to the fixing time itself. Ordinary cold tap water is commonly used, and it may be allowed to circulate gently in the vessel containing the fixed plates. The hypo remaining in the emulsions must be completely removed to prevent later fading of the developed image, since the sulfur of the hypo ultimately combines with the image silver to give silver sulfide. Adequate washing is therefore necessary. A simple indicator solution for testing used wash water for the presence of hypo is given in Table 3–III. Several drops of this solution, ordinarily violet in color, when added to a sample of water containing hypo will turn

orange in less than a minute, with large hypo concentrations resulting in a yellow coloration.

Drying

Drying nuclear emulsions subsequent to their washing requires care if the gelatin is not to be distorted. Since the evaporation of water from the surface of the emulsion is ordinarily much more rapid than the outward diffusion of water from the interior, to avoid strains it is necessary to maintain a humid atmosphere during the drying. The exact procedure involved varies with the laboratory, the most usual methods requiring several days at about 90 percent relative humidity followed by several days further at lower humitities. Blowing over the surface of the emulsions during drying is to be avoided since it introduces severe distortion (Dainton *et al.*, 1951), although the temperature may be increased somewhat to accelerate the process. Dilworth (1951) has pointed out that the edges of the plate usually dry first, causing surface deformation of the emulsion. This can be remedied almost completely by surrounding the plate with a "guard ring" of other similar plates edge-to-edge, which results in much more even drying.

Plate Preservation

When drying has been completed it is usually advisable to treat the emulsions further in order to prevent their peeling from the glass supports. This is especially necessary with thick emulsions, although it may not be required at all for thin ones (<200 microns) if a plasticizing bath is used before drying. Coating the plate edges with clear shellac or lacquer suffices in most cases for Ilford emulsions, which seem to adhere better than those manufactured by Eastman. For the latter plates and for plates 600 microns or more in thickness the entire emulsion surface as well as the edges should be sprayed with a suitable coating. Under circumstances where peeling and cracking occur despite these precautions, as in the case of frequent or rapid temperature and humidity changes, thin microscopic cover glasses may be cemented to the emulsion surface with gum damar dissovled in Xylene (Stelson, 1950).

3-2. TEMPERATURE DEVELOPMENT

As a consequence of the time required for the developing solution to penetrate thick emulsions, the halide grains near the surface will ordinarily be developed to a greater extent then those near the glass-emulsion interface. Tracks incident at an angle to the emulsion plane would be unequally developed along their lengths, rendering grain density determinations impossible, and events occuring at different depths could not be compared with each other. To overcome this difficulty Dilworth, Occhialini, and Payne (1948) devised the "temperature development" procedure in which the emulsion is placed in developer at a temperature sufficiently low to inhibit its action until it has permeated the entire emulsion. The developer is then warmed, permitting it to act on the emulsion. A similar method is employed to stop the development, the temperature being reduced rapidly by immersion in a cold stop bath.

TABLE 3-III. Formula for hypo indicator solution.

Distilled water	180 ml
Potassium permanganate	0.3 g
Sodium hydroxide	0.6 g
Distilled water to make	250 ml

Presoaking

To facilitate penetration, presoaking in distilled water with or without the addition of a wetting agent is frequently done. This acts to swell the gelatin, permitting more rapid diffusion of the developer, but will not affect the actual development as will alkaline solutions (Dilworth *et al.*, 1948; Mortier and Vermassen, 1948; Picciotto, 1949). The temperature at which penetration is to occur is usually chosen in the neighborhood of 5°C, since above that temperature the rate of developer penetration increases less rapidly than its activity does and below that the penetration time becomes unduly long.

Development

When the emulsion has been saturated with the cold developer, the temperature may be raised to permit the development process to occur. At this point it is necessary that no additional fresh developer enter the emulsion, because this also would result in uneven development. There are three methods of accomplishing this in general use at present: developer dilution, dry development, and mechanical protection of the emulsion surface. The first of these requires a rather critical adjustment of the developer concentration to prevent either the inward diffusion of fresh developer into the emulsion or the outward diffusion of the developer already there. The usual practice involves the dilution of one part of the developer at the concentration which was permitted to permeate the emulsion when cold with two parts distilled water, and, although unsuited to really precise work, this procedure requires a minimum of manipulation. In dry development (Dilworth *et al.*, 1951; Dainton *et al.*, 1951) the plates are removed from the developing bath, the excess solution on their surfaces removed with filter paper or other appropriate absorbent material and then brought to the selected developing temperature and maintained there. The latter is most conveniently accomplished by placing the plates glass downward on a heated surface, care being taken to insure good thermal contact. A temperature between 25° and 30°C may be employed, reducing the time ordinarily required for this step considerably. Temperatures of the order of 20°C are usual for development in the solution itself. While with this technique any overdevelopment of the upper part of the emulsion is avoided, developer oxidation

in this region may occur, leading to underdevelopment. Such oxidation may be avoided by introducing an inert gas into the container in which the plates are being heated. The third method, involving the physical covering of the emulsion, is accomplished by means of glass plates covered with wax to prevent their adhering to the emulsions or, alternatively, by the use of oil to cover the emulsion surface. In the latter case it is necessary to remove all traces of the oil before immersion in the stop bath.

With emulsions of considerable thickness (greater than 1 mm) it may be necessary to employ additional methods of restraining the action of the developer until adequate penetration has occurred. In addition to further reducing the temperature, which may necessitate the use of antifreezing agents, it is possible to add more bromide to the developers than the formulas ordinarily call for, which requires lengthening the developing time to compensate for the reduction in the velocity of development. Changing the *p*H of the developer will have the same effect, with the time of development increasing with the acidity of the solution. Amidol developers are especially adapted to this technique, working well in acid conditions (Dilworth *et al.*, 1951).

Some specific processing instructions for both development in solution and dry development, as well as the pertinent formulas, are to be found in Tables 3–II, 3–IV, and 3–V.

Reticulation

Reticulation is a severe distortion of the emulsion produced by irregular swelling and shrinkage of the gelatin. In the processing of nuclear emulsions it usually occurs in the transfer of plates from cold solutions to ones at higher temperature without sufficient time being spent at intermediate temperatures. Reticulation involves the movement of the silver particles comprising the visible image as well as the production of a wrinkled surface (Mees, 1942), with the silver tending to concentrate in the ridges of gelatin. An extreme degree of reticulation is sufficient to render useless any plates exhibiting it, and even moderate reticulation impairs in accuracy the track measurements. The gradual raising of solution temperatures or the use of a sufficient number of intermediate baths permits the processing of plates showing no sign of this distortion, and these procedures are necessary for best results with the temperature development method.

3–3. PENETRATION OF DEVELOPER

The various aspects of the penetration of developers in nuclear emulsions have been very thoroughly investigated by Dainton, Gattiker, and Lock (1951) at Bristol. Employing Ilford G5 emulsions of various thicknesses with four developing agents with and without presoaking in distilled water, their results establish a quantitative basis for development procedures involving the temperature method. To determine penetration times the emulsions were exposed through their glass backings to a characteristic image from a photographic enlarger in such a way that only a layer approximately 3 microns thick at the glass-emulsion interface had a latent image produced in it. The emulsions were then developed, the penetration time being taken as the time for a clearly defined image to appear.

TABLE 3-IV. Processing procedure for 100- and 200-micron emulsions recommended by Eastman Kodak.

Procedure	Temperature	Time
Developer penetration (D19 diluted 1:1)	5°C.	30 minutes
Development (2 parts water at 20°C added)	20°C	30 minutes
Acid stop bath (2%, nitrogen agitation)	5°C	30 minutes
Fixation (30% hypo)		
Penetration	5°C	15 minutes
Fixation (nitrogen agitation)	20°C	5 minutes longer than clearing time
Wash (running water)	10°C	1 hour minimum

The nominal and actual thicknesses before processing of the emulsions used are given in Table 3–VI. The preliminary soaking in distilled water was for a period of three hours in all cases, and in all cases reduced considerably the time required for penetration. The results obtained for the penetration times with Azol, D19b, Amidol (a), and Amidol-bisulfite developers at 20°C are given in Table 3–VII for two sets of plates, one of which was presoaked and the other not. The ratios of the average penetration times for the two sets were, for Azol, 1.34; for D19b, 1.70; for Amidol, 1.86; and for Amidol-bisulfite, 1.65. Penetration time measurements of presoaked emulsions at 5°C, 10°C, and 15°C were also made with the use of only Azol, D19b, and Amidol, since Amidol and Amidol-bisulfite had virtually identical penetration times at 20°C. These are given in Table 3–VIII, with the results for 20°C being included for convenience. It is possible to express these results for a given developer and temperature by the formula

$$T = kt^x, \tag{3–1}$$

where T is the penetration time, t the thickness of the emulsions, x a number of the order of 1.4, and k a constant depending upon the developer and the temperature.

3–4. TWO-BATH DEVELOPMENT

In another approach to the problem of securing the even development of thick emulsions, Blau and De Felice (1949) employ two developer solutions. The first

contains the developing agents without any alkali, permitting diffusion of the developer into the emulsions without any appreciable amount of actual development occurring. The second bath, containing an excess of alkali, permits the development to take place. This method requires that the velocity of travel of a *p*H change exceed that of the developer itself, a condition that is not actually satisfied (Dainton *et al.*, 1951). However, for emulsions of up to perhaps 400-micron thickness the two-bath method eliminates any danger of emulsion reticulation which frequently occurs in the temperature development procedure unless elaborate precautions are taken. Table 3–IX contains the details of the two-bath method.

Developer Distortion

There are a number of applications of nuclear emulsions in which the absence of any distortion whatever is of paramount importance, rather than even development throughout the emulsion depth. Such an application would be, for example, the magnetic deflection of particles in air gaps between two plates (Sec. 4–6). The temperature method of processing thick emulsions, while producing the most even development, also gives the greatest degree of distortion (Barbour, 1950). This may be attributed to shocks due to the temperature change undergone by the emulsions during the various processing steps, which, although they may be minimized by careful handling, cannot be altogether eliminated. The two-bath method results in much less distortion probably by virtue of the constant temperature employed, but an increased density of background and surface grains is also present. This renders accurate determinations of points of entry into the emulsion very difficult, and, of course, the emulsion surface cannot be wiped to eliminate the surface deposit lest further uncertainty result. Barbour found that using a more dilute developer at a lower temperature than usual would reduce distortion to a minimum, while at the same time not creating too great a development gradient. With 4:1 D19 at 18°C approximately 55 minutes were required to develop 200-micron emulsions, the diffusion time thus being a smaller part of the total time spent in the developer than in the case of a more concentrated solution at 20°C.

3–5. PELLICLES

Pellicles, nuclear emulsion films without any glass backing, present something of a problem in processing due to their appreciable (~25 percent) amount of sublateral swelling while immersed in solution with the subsequent danger of severe distortion. In addition, the wet emulsions are extremely fragile and must be treated with care to prevent their adhering to their containers. Ordinarily the pellicles are supported at one end by stainless steel clips during processing. Processing instructions for Eastman Kodak 250-micron pellicles

TABLE 3-V. Processing procedure for 400- and 600-micron emulsions of Nucleonics Division, Naval Research Laboratory, Washington, D. C. (Stiller, 1951a).

Procedure	Temperature	Time
Presoaking (distilled water)	ambient→5°C	100 min
Developer penetration (Amidol (b))	5°C	100 min
Dry development	23°C	20 min
Dry cooling	23°C→8°C	5 min
Acid stop bath (1%)	5°C	100 min
Removal of surface deposit		
Fixation		
Clearing	5°C	18 hours
Dilution	5°C	24 hours
Washing	5°C	24 hours
Plasticizing solution (10% Ansco "Flexogloss")	5°C	30 min
Drying (rel. humidity 100%→50%)	21°C	7 days

are given in Table 3–X. After washing is completed, the pellicles are placed on glass plates somewhat larger than their own size. These plates should have gelatin coatings, either special plates supplied by the manufacturer or undeveloped but fixed and washed nuclear emulsion plates being suitable. The pellicles on their glass backings are then placed in a refrigerator and kept there until they have set. Drying is then conducted at 20°C.

An alternative method of processing pellicles has been employed by Stiller *et al.* (1951) based upon a suggestion by C. Waller. This involves the mounting of the pellicles on glass backings before processing, rather than afterward as above. The mounted pellicles are then processed exactly as any orthodox plate of their emulsion thickness, no special precautions being necessary. Of course, in this way no advantage is taken of the rapid development and fixation possible with unsupported emulsions as a result of the permeation of solutions from both surfaces, but distortion is reduced by a considerable extent.

3–6. SHRINKAGE

The high concentration of silver bromide in nuclear emulsions will result in a considerable reduction in their thickness after fixation, when the unused silver is removed. If the ratio between the thicknesses of one emulsion before and after processing, which is the "shrinkage factor," is known, it is possible to correct for this effect

TABLE 3-VI. Emulsion thicknesses.

Nominal	Actual
100 microns	105 microns
200 microns	230 microns
300 microns	260 microns
400 microns	400 microns
600 microns	675 microns
800 microns	720 microns
1000 microns	1050 microns

TABLE 3-VII. Penetration times at 20°C in presoaked and non-presoaked emulsions.

Developer	Penetration time in minutes for different thicknesses 105m	230m	260m	400m	675m	720m	1050m
Azol							
Presoaked	4.5	17	22	38	96	96	210
Non-presoaked	6	21	27	50	138	123	330
D19b							
Presoaked	3.5	9.5	14.5	21	50	64	140
Non-presoaked	5	12	20	37	110	125	270
Amidol							
Presoaked	1.5	6	8.5	12	26	26	58
Non-presoaked	3.5	9.5	11.5	22	49	52	120
Amidol-bisulfite							
Presoaked	2	6.5	8	12	25	25	55
Non-presoaked	2	8.5	10	20.5	53	46	110

in determining track lengths by using the formula

$$R=[Y^2+(SZ)^2]^{\frac{1}{2}}, \tag{3-2}$$

which gives the original (i.e., before processing) length R of a track in terms of S, the shrinkage factor, and Y and Z, its horizontal and vertical components as measured subsequent to processing. An exception to this equation occurs in the case of heavy particles with large ($>25°$) angles of dip in the emulsion (Rotblat and Tai, 1949, 1951), with these tracks exhibiting a smaller relative decrease in angle than those incident at smaller angles. This is evident from Fig. 3–2, which gives the calculated track lengths as functions of dip angle for triton+alpha tracks from lithium disintegrations in C2 emulsions (Sec. 4–3). The difficulty of moving grains which come in contact with each other during the shrinking, preventing them from following the displacement of the gelatin surrounding their positions, is most likely the cause of this effect. Rotblat and Tai give as the equation for the critical angle θ_0, the angle at which deviations from Eq. (3–2) first occur,

$$\cos\theta_0=\left[\frac{S^2-\{R/(R-l)\}^2}{S^2-1}\right]^{\frac{1}{2}}, \tag{3-3}$$

TABLE 3-VIII. Penetration times at various temperatures in presoaked emulsions.

Developer	Temperature	Penetration time in minutes for different thicknesses 105m	230m	260m	400m	675m	720m	1050m
Azol	5°C	11	45	50	100	270	300	300
	10°C	8.5	27	34	70	185	208	210
	15°C	8.5	25	30	63	145	150	210
	20°C	4.5	17	22	38	96	96	210
D19b	5°C	6	21	27	58	165	172	270
	10°C	5	16.5	19	37	108	115	210
	15°C	4	12	17	27	72	68	220
	20°C	3.5	9.5	14.5	21	50	64	140
Amidol	5°C	5	16	20	37	80	84	190
	10°C	3.5	11	13.5	22	51	53.5	110
	15°C	3	8	11.5	18	37.5	45	95
	20°C	1.5	6	8.5	12	26	26	58

TABLE 3-IX. Two-bath development.

Solution A:

Elon	1.1 gram
Sodium sulfite	24.0 gram
Hydroquinone	4.4 gram
Potassium bromide	2.0 gram
Distilled water to	2 liters

Solution B:

Stock Eastman D19	400 cc
Distilled water	1600 cc
Sodium carbonate	16 gram

Procedure:

1. Presoak for 10 min in distilled water.
2. Solution A for 30 min (slight agitation).
3. Solution B for 30 min (no agitation).
4. 2% acetic acid for 15 min (agitation).
5. Eastman F5 fixing-bath 6–8 hours at 74°F (agitation).
6. Wash in running water 2 hours.

where R is the range and l the total vacant space in horizontal tracks.

Shrinkage Factor

Ideally, the shrinkage factor should be given by

$$S=1+V_s/V_g, \tag{3-4}$$

where V_s is the volume of the soluble material and V_g the volume of the remaining gelatin. However, it is necessary to take into account the variation in S with the humidities prevailing during the exposure of the emulsion and during its observation subsequent to processing, since the proportion of moisture present will be different for processed and unprocessed emulsions. Figure 3–3 gives the moisture content a_0 of processed and a_e of unprocessed emulsions in terms of the ratio between the volumes of water and the volumes of gelatin present at various relative humidities. The

TABLE 3-X. Processing procedure for Eastman Kodak 250-micron pellicles.

Procedure	Temperature	Time
Permeation of developer (D19b)	5°C	10 min
Development (add 2 parts water at 20°C)	20°C	10 min
Acid stop bath (2%) (agitation)	5°C	10 min
Fixation (30% hypo)		
Permeation	5°C	10 min
Fixation	20°C	5 min longer than time to clear
Wash	15°C	Fixing time
Alternate Procedure		
Development (D19b) (agitation)	20°C	8 min
Acid stop bath (2%) (agitation)	20°C	5 min
Fixation (30% hypo) (agitation)	20°C	Twice time to clear
Wash	15°C	Fixing time

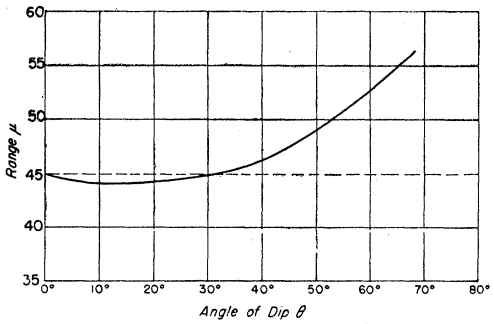

FIG. 3–2. Calculated track lengths as a function of dip angle for triton+alpha-particle tracks from lithium-slow neutron disintegrations (Rotblat and Tai, 1951).

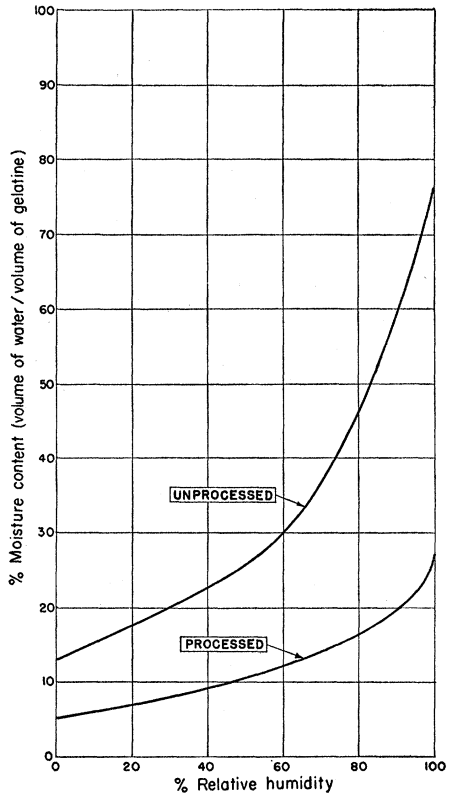

FIG. 3–3. The moisture contents of Ilford emulsions before and after processing. The curves were calculated from the emulsion composition in the former case and experimentally determined in the latter (Rotblat and Tai, 1951).

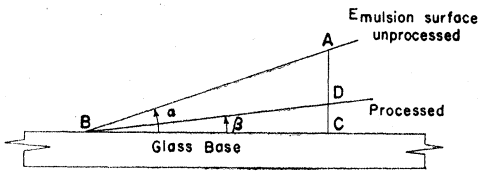

FIG. 3–4. Emulsion wedge before and after processing (Roads, 1951).

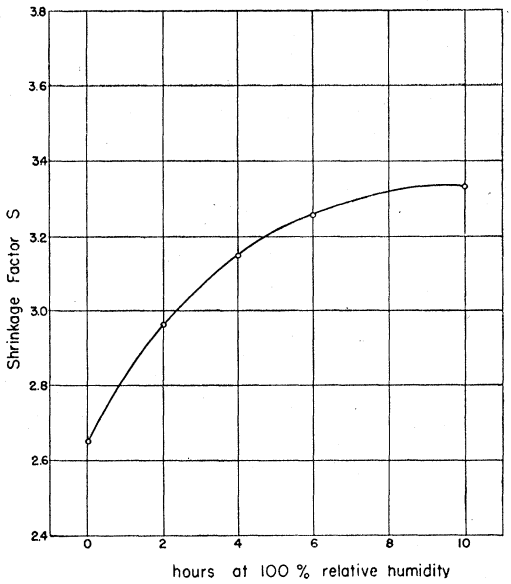

FIG. 3–5. The increase in the shrinkage factor in Ilford G5 emulsions with time of storage at 100 percent relative humidity (Roads, 1951).

empirical formula

$$S=\frac{S_0+1.27a_e}{1+a_0} \tag{3–5}$$

gives the shrinkage factor as a function of the water contents of the emulsion, which may be expressed in terms of humidity measurements with the aid of Fig. 3–3. The quantity S_0 is the shrinkage factor for an absolutely dry emulsion and is about 2.22 for Ilford emulsions.

The usual methods of determining S experimentally have involved either direct measurements of the difference in depth between the highest and lowest fog grains visible by means of the calibrated fine adjustment of the microscope or the use of a technique due to Vigneron (1949). The latter makes use of Eq. (3–2), with Y and Z for tracks of the alpha-particles from ThC′ being measured. Since R for these tracks is a constant, a graph of Y^2 *versus* Z^2 for tracks of varying angles of dip will give a straight line of slope equal to S^2. A particularly elegant and accurate method of determining S has been devised by Roads (1951), making use of optical interference patterns. If the emulsion is coated on its glass backing in a wedge form, the angle α made by the surface of the emulsion with the glass may be determined very exactly from the width x of the fringes produced between the plate and an optical flat with monochromatic light. After processing the wedge will exhibit a smaller angle β corresponding to a fringe width x'. From Fig. 3–4,

$$S=AC/DC=\tan\alpha/\tan\beta \tag{3–6}$$

and, since

$$\tan\alpha=\lambda/2x \tag{3–7}$$

and

$$\tan\beta = \lambda/2x', \tag{3-8}$$

where λ is the wavelength of the light used, S may be determined directly from the relation

$$S = x'/x.$$

In practice, a single plate was used to determine simultaneously both fringe widths by having part of it processed and part left unprocessed, the line separating the two regions being perpendicular to the slope of the wedge. The results of this investigation give $S = 2.38 \pm 0.04$ and 2.65 ± 0.07 for Ilford C2 and G5 emulsions, both at normal room humidity. These figures are in accord with those of Rotblat and Tai. Roads has also evaluated the change in S with time of storage in a saturated atmosphere, his results being given in Fig. 3–5.

In cosmic-ray work a measurement of shrinkage is possible when a well-aligned stack of plates is exposed in the upper atmosphere. Energetic heavy primaries will penetrate the entire stack and their angle of incidence can be determined from their positions in successive plates. This angle and that measured in the emulsion will permit S to be determined.

Chapter 4. Auxiliary Techniques

4–1. BACKGROUND ERADICATION

In a great many applications it is necessary to remove the accumulated background tracks ordinarily present in nuclear emulsions prior to their exposure. Such tracks are, for the most part, due to the decay of radioactive contaminants such as thorium present both in the emulsions and their glass backings, although some of the background may be caused by cosmic radiation if the plates have been transported by air. Storage in the vicinity of particle accelerators for even a brief period may produce significant background largely a result of fast neutron recoils and, in the case of electron-sensitive emulsions, gamma-radiation.

Photographic latent images may be oxidized rather easily, and this property is made use of in the various techniques that have been proposed for background eradication. Direct immersion of the plates in oxidizing solution has been attempted by Perfilov (1944a, b) and Powell *et al.* (1946) with chromic acid in concentrations up to two percent. While this treatment is effective in removing background tracks, it also renders the emulsions insensitive to protons and lighter particles. The sensitivity to alpha-particles and fission fragments, while decreased, is nevertheless sufficient after treatment with chromic acid to permit the use of the plates for recording these particles.

A more satisfactory method has been proposed by Yagoda and Kaplan (1948). Hydrogen peroxide is used as the oxidizing agent here and the emulsions are exposed to its action by suspending them above a three percent solution at 25°C. A treatment of three to four hours is sufficient for 25- and 50-micron emulsions, while much longer periods are required for thicker emulsions. After the eradication the plates must be dried thoroughly, with care being needed since peeling occurs if the drying is overly rapid. The principal objection to the use of hydrogen peroxide is that, with thick emulsions, the times necessary (>15 hours) are such that partial desensitization again becomes a problem. Furthermore, this desensitization is not uniform throughout the emulsion volume.

Wiener and Yagoda (1950), in a more recent suggestion, advocate water vapor as being effective and at the same time producing a minimum loss of sensitivity. Ilford C2 emulsions of 200-micron thickness were exposed to air saturated with moisture at a temperature of 35°C for 16 hours, drying being done over anhydrous calcium chloride for one hour. The tracks of low energy protons and of alpha-particles are not affected by this treatment, but some desensitization may be expected with lightly ionizing particles such as fast protons and mesons. However, at present this procedure seems the best that can be done in this direction.

4–2. LIMITATION OF SENSITIVE TIME

One of the major limitations at present of nuclear emulsion technique lies in the continuous sensitivity of the emulsions. This renders unknown the circumstances (e.g., time, place) attendant upon the recording of particular phenomena. For example, in studying cosmic radiation in the upper atmosphere with plates the exact time and altitude at which various specific events have occured cannot be determined, although, of course, differences in the frequency of occurance of certain phenomena under different circumstances may be inferred on a statistical basis. Indeed, since emulsions retain all events that have been recorded from their manufacture until their processing, it is usually impossible on other than probability considerations to determine whether or not the events in question have even occurred during the period of investigation. In view of these circumstances it would be of great value if practical techniques for the limitation of the sensitive time of nuclear emulsions could be developed.

Thermal Methods

Thermal methods of controling the sensitive time making use of the variation of emulsion sensitivity with temperature (Sec. 1–4) have been proposed in the past (Dilworth, 1949), but these are of only limited utility. The primary reason for this lies in the fact that the minimum sensitivity attainable in the laboratory for a given emulsion, employing liquid nitrogen, is only about one-third that at the optimum exposure temperature, 20°C. In addition, the most sensitive emulsions (Ilford G5, Kodak NT4, Eastman NTB3) experience an even smaller reduction at low tempera-

tures. It is therefore unlikely that effective exposure control can be obtained on the basis of a thermal technique.

Desensitizer Method

An alternate procedure (Beiser, 1950a) makes use of the dependence of the action of certain photographic desensitizing agents on oxygen concentration (Blau and Wambacher, 1934). The dyes used for this purpose apparently act as catalysts for the oxygen in its reaction with the silver bromide grains of the emulsion, and are capable of preventing the formation of latent image while not ordinarily adequate to attract an existing one. These desensitizers (phenosafranine, pinakryptol yellow, and pinakryptol green) presumably act to compete with the sensitivity specks of the bromide grains in trapping electrons emitted during irradiation. Preliminary investigation indicates that the use of this approach does succeed in accomplishing sensitivity limitation, the procedure being to desensitize the emulsions initially and expose them by either lowering the pressure of the air around them or by replacing the air by an inert atmosphere. Further quantitative information is necessary, however, before this technique can be put to practical use.

4–3. NEUTRON DETECTION

Neutrons, being uncharged, are not susceptible to direct recording in nuclear emulsions. They may, however, be detected in a number of indirect ways by use of these emulsions, the principal ones involving the observation of proton recoil tracks and emulsion impregnation with substances acted upon by neutrons to produce characteristic phenomena.

Another technique, utilizing ordinary photographic emulsions, has been developed by Kallmann (1948). This method makes use of the production of heavily ionizing particles such as tritons and alpha-particles when slow neutrons are incident upon Li^6 or B^{10} (see below), these particles then activating suitable phosphors with the resulting light being recorded on photographic plates. The best arrangement for this purpose consists of an emulsion covered with a phosphor layer, a thin film of aluminum foil to reflect the greater part of the fluorescent light into the emulsion, and a layer of lithium or boron. For fast neutrons the latter layer may be replaced by one of paraffin, with recoil protons activating the phosphor.

Slow Neutrons

For the detection of slow neutrons a number of reactions may be employed by loading a nuclear emulsion with a compound of an appropriate substance. Details of the latter procedure are given in Sec. 4–5, and the commercial availability of loaded emulsions is also discussed there. The two reactions most commonly made use of are

$$Li^6+n^1\rightarrow He^4+H^3, \qquad (4\text{–}1)$$

and

$$B^{10}+n^1\rightarrow Li^7+He^4. \qquad (4\text{–}2)$$

The Li^6 disintegration produces distinctive tracks about 40 microns long, depending upon the stopping power of the emulsion, due to the alpha-particle and triton products being ejected in opposite directions (Burcham and Goldhaber, 1936; Demers, 1947; Allred *et al.*, 1950). These tracks are unusual in that they increase in grain density in both directions from a point about 6 microns from one end, corresponding to the location of the B^{11*} compound nucleus. The range distributions of the decay particles from this reaction have been determined by Allred *et al.* for Ilford C2 emulsions and are given in Fig. 4–1.

The alpha-particle tracks from the B^{10} reaction are less conspicuous than those resulting from Li^6 disintegrations, the majority being in the vicinity of 4 microns long corresponding to an energy of 1.6 Mev. The lithium nucleus recoils with an energy of 0.9 Mev but has a very short range due to its comparatively large mass. However, the cross section for the boron reaction is several times greater than that for the lithium one, rendering it more useful for low neutron intensities. In Fig. 4–2 the range distribution in Ilford C2 emulsions of the alpha-particles from B^{10} is shown, the peak at slightly less than 4 microns being the result of an excited state in Li^7.

It must be kept in mind that commercial boron contains only about 20 percent of the B^{10} isotope, the remainder being B^{11} which does not react with slow neutrons, although "enriched" boron, containing up to about 96 percent B^{10}, may be obtained. Similarly, ordinary lithium is composed of 7.5 percent Li^6 and 92.5 percent Li, higher concentrations of Li also being possible upon enrichment. Impregnation with lithium borate (Yagoda, 1949) may be used to combine the effects of both the above reactions. Details of this procedure are given below.

Another reaction sometimes employed is

$$N^{14}+n^1\rightarrow C^{14}+H^1, \qquad (4\text{–}3)$$

which results in proton tracks of about 7 microns in length (Cheka, 1948). This means of slow neutron detection is limited both by the small cross section of the process and by the low nitrogen content of the emulsion gelatin. For studies involving the use of this method the emulsion can be impregnated with nitrogen-rich compounds such as sodium azide (Cüer, 1947). Uranium loadings in nuclear emulsions give fission tracks resulting from U^{235} slow neutron capture (Lark-Horovitz and Miller, 1941). Alternatively, thin uranium foils may be exposed to neutrons while in contact with appropriate emulsions (Froman *et al.*, 1947).

Fast Neutrons

Fast neutrons may be identified by the recoil or knock-on protons they produce by collision with the hydrogen atoms of emulsions (Powell, 1940, 1943;

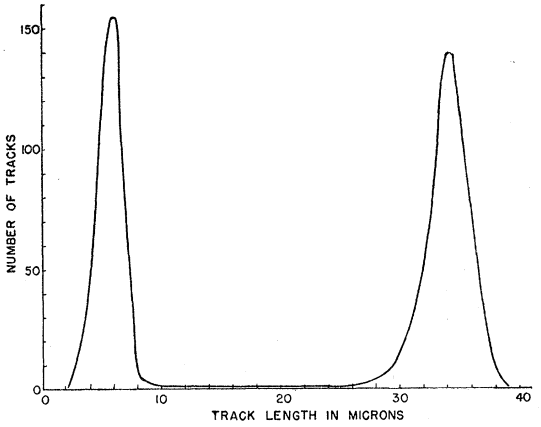

FIG. 4–1. Range distributions in Ilford C2 emulsions of alpha-particles (shorter tracks) and tritons from the disintegration of Li^6 by slow neutrons (Allred *et al.*, 1950).

Gibson and Livesey, 1948; Livesey and Wilkinson, 1948; Grosskreutz, 1949; Allred *et al.*, 1950; Nereson and Reines, 1950). Heavier nuclei also undergo neutron collisions, but the energy transferred is not sufficient for them to produce perceptible tracks. This is evident from the expression for the recoil energy E in terms of E_n, the original neutron energy, θ, the angle between the trajectory of the recoil and the line of flight of the incident neutron, and M, the mass number of the recoil nucleus, here assumed to be initially at rest

$$E=[4M/(1+M)^2](E_n\cos^2\theta). \tag{4–4}$$

The maximum value of E will occur for $\theta=0$, a direct head-on collision, when

$$E=[4M/(1+M)^2]E_n. \tag{4–5}$$

A complete transfer of energy, $E=E_n$, is possible only when $M=1$, i.e., for a neutron-proton collision. The possibility of neutron-neutron collisions is not present in this case. It is apparent that the recoil energies of the heavier nuclei present in the emulsion will be very much smaller than those for hydrogen, any observable recoils almost certainly being due to the latter. The recoil proton energies are related to the original neutron energies by

$$E=E_n\cos^2\theta, \tag{4–6}$$

the average fractional energy loss being $1/e$ or about 0.37 in each encounter.

In the interpretation of recoil tracks it must be remembered that neutrons may be scattered through small angles by heavy nuclei while retaining virtually their entire original energies. These neutrons will give energetic protons recoiling with larger share of the initial neutron energies than might be expected from the values of θ that are present. If such protons are interpreted as resulting from collisions with unscattered neutrons, the energy determinations may be somewhat in error. In the investigation of neutron energy spectra it is therefore advantageous where possible to use a source of recoil protons separate from the emulsion used as the detector, since experimental geometries may then be employed which permit unambiguous energy determinations. An example of an arrangement making use of a thin polythene scatterer is given in Fig. 4–3 (Allred *et al.*, 1950). In addition, such a technique greatly facilitates scanning, since only the emulsion surface need be examined for the proton tracks.

Boron loadings may also be used for fast neutron detection by utilizing the reactions

$$B^{10}+n^1\rightarrow He^4+He^4+H^3, \tag{4–7}$$

and

$$B^{11}+n^1\rightarrow Li^8+He^4. \tag{4–8}$$

The alpha-particles and the triton from the B^{10} reaction form a three-pronged star, the sum of their energies approximating that of the incident neutron (Lattes and Occhialini, 1947). The B^{11} events may be identified by the "hammer track" resulting from the subsequent decay of Li^8 into two alpha-particles (Pickup, 1948). The energy of the initially emitted alpha-particle is 5.4 Mev, that of the Li^8 nucleus 1.7 Mev, and the total energy of both alpha-particles from the decay of the latter is 2.6 Mev. If electron-sensitive emulsions are used the beta-decay of Li^8 into Be^8 prior to the production of the alpha-particles may also be observed.

The possibility of employing the reaction

$$Li^6+n^1\rightarrow He^4+H^3 \tag{4–9}$$

in the detection of fast as well as slow neutrons has been investigated by Keepin and Roberts (1949, 1950). The chief advantage of this technique is that it does not require a collimated neutron beam. The cross section for the disintegration of Li^6 by fast neutrons is only about 0.1 barn, ten times smaller than that for proton recoils, but loading emulsions with enriched lithium having a greater percentage of Li^6 than ordinary lithium somewhat compensates for this bad feature. Distinguishing between the alpha-particle and triton tracks may be facilitated by the use of standard track

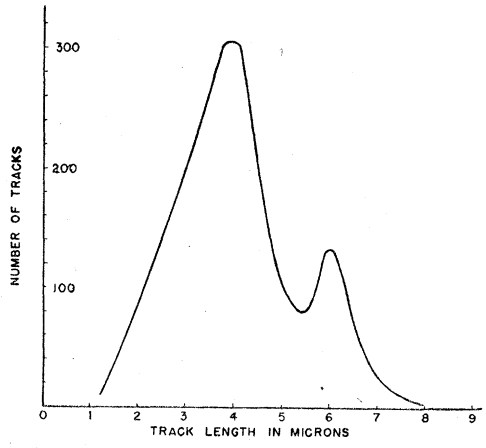

FIG. 4–2. Range distribution in Ilford C2 emulsions of alpha-particles from the disintegration of B^{10} by slow neutrons (Allred *et al.*, 1950).

discrimination methods. In practice, both the sum of the lengths of the two tracks and the angle θ between them is measured. The energy of the incident neutron is then determined from curves such as those in Fig. 4–4, which gives the neutron energy as a function of total range of the tracks for various values of θ. For any given neutron energy there are two possible total ranges, corresponding to the cases in which the triton is favored in the energy distribution, resulting in the larger total range, and the alpha-particle is favored, giving the smaller range. The ranges in Fig. 4–4 apply to Ilford C2 and Eastman Kodak NTA emulsions and may have to be corrected for emulsions of different stopping power.

4–4. GAMMA-RAY SPECTRA

The photodisintegration of the deuteron provides a convenient and very accurate method for determining the energy spectra of gamma-rays with deuterium-loaded emulsions (Powell, 1940; Gibson, 1947; Bosley, Craggs, and Nash, 1948; Goldhaber, 1948, 1950; Wäffler and Younis, 1949, Wang and Weiner, 1949; Miller *et al.*, 1950; Hough, 1950; Krohn and Shrader, 1951). The photon energy is given by the sum of the binding energy of the deuteron, 2.18 Mev, and the energies of the proton and neutron products. Since the latter are equal, a knowledge of the proton energy alone is sufficient. Details of loading with deuterium are given in Sec. 4–5.

A more accurate energy determination is possible when the direction of the incident gamma-ray beam is known, as in the calibration of a betatron. Krohn and Shrader (1951) have given the photon energy E in this case as

$$E=\frac{2E_p+W}{1-(2E_p/m_1c^2)+(4E_p/m_1c^2)^{\frac{1}{2}}\cos\theta}, \quad (4\text{–}10)$$

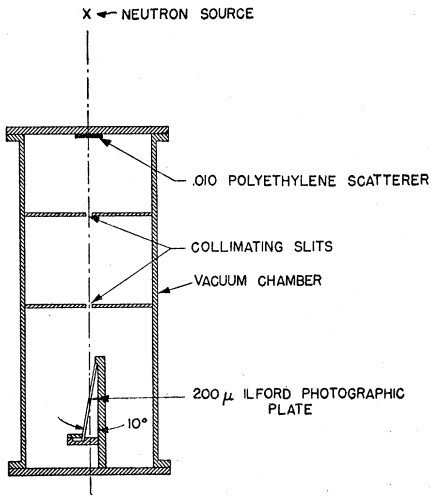

FIG. 4–3. Experimental arrangement for the determination of neutron energy spectra (Allred *et al.*, 1950).

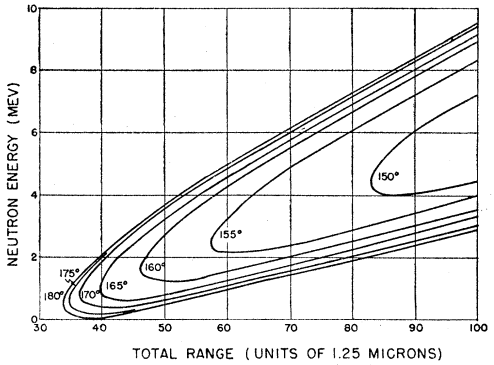

FIG. 4–4. Neutron energy as a function of the total range in emulsion (in units of 1.25 microns) of the alpha-particle and triton products from the disintegration of Li^6 for various values of θ (Keepin and Roberts, 1949).

where E_p is the proton energy as determined from its range in the emulsion, θ the space angle between the foreward directions of the proton track and the beam, m_1 the deuteron mass, and $W=(m_2+m_3-m_1)c^2$ where m_2 and m_3 are the proton and neutron masses. A series of curves of constant E_p plotted against θ and E is given in Fig. 4–5, which enables the evaluation of E from the known angle and energy of a photoproton.

A number of other nuclear photodisintegration processes exist which may be considered for certain gamma-ray determinations, although in general they are strongly endoergic and have relatively low cross sections for such reactions. Two processes that have been suggested (Yagoda, 1949) for such use are

$$Be^9+\gamma\rightarrow 2He^4+n^1 \quad (4\text{–}11)$$

and

$$C^{12}+\gamma\rightarrow 3He^4. \quad (4\text{–}12)$$

That the former reaction is more probable than the production of photoneutrons, which would leave a Be^8 residual nucleus, has been shown by Glückauf and Paneth (1938). The disintegration of C^{12} requires 7.16 Mev, and three-pronged alpha-particle stars have been observed that are attributed to this process (Hänni *et al.*, 1948).

4–5. IMPREGNATION

The usefulness of nuclear emulsions can be greatly extended by impregnating (loading) them with particular substances whose properties or reactions are to be studied. This method provides a convenient means for investigating the radioactivity of long-lived alpha-emitters such as samarium, and makes possible neutron detection by loading with lithium or boron. Yagoda (1949) has gone into various aspects of impregnation in some detail.

General Considerations

Loading with a given substance is usually accomplished by immersing an emulsion in the appropriate

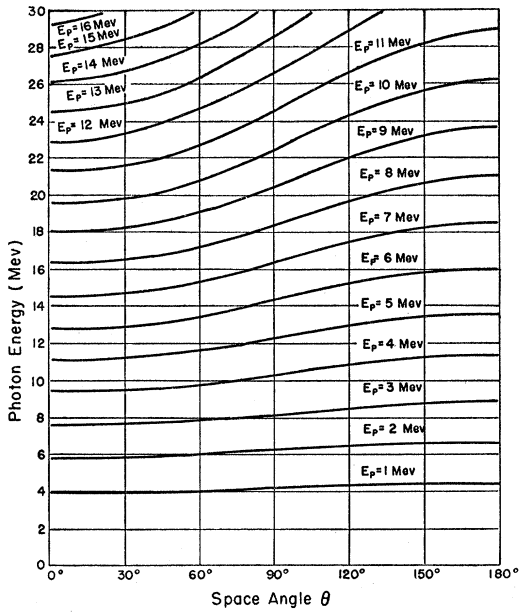

FIG. 4–5. Proton kinetic energy as a function of photon energy and space angle in the photodisintegration of the deuteron (Krohn and Shrader, 1951).

solution for a length of time dependent upon the concentration of the substance in the solution, the desired concentration in the emulsion, the emulsion thickness, and the temperature. This is followed by a very brief water rinse to remove the solution adhering to the emulsion surface, and the plate is then allowed to dry in a dust-free atmosphere. The precise quantity of the adsorbed material may be determined either by analyzing the resulting loaded emulsion or, knowing its concentration, by measuring the volume of solution removed by the emulsion.

An alternate method, usually giving a less uniform distribution of the foreign substance, consists in placing a quantity of the solution on the emulsion surface and allowing it to evaporate to dryness. The advantages of such a procedure are that the amount of added material is known precisely and that only a minimum of solution is required. About 1 ml of solution is sufficient for a 40 cm^2 emulsion area. It is desirable to use a volatile solvent such as alcohol to make evaporation more rapid, and perhaps a small quantity of wetting agent to facilate uniform spreading.

A number of substances, such as chromates and uranyl ions, tend to desensitize emulsions in which they are incorporated (Green and Livesey, 1946; Broda, 1947). Other heavy ions, lead and bismuth for example, also result in partial desensitization (Broda, 1946). If the alpha-emitting properties of an element are being studied it is not undesirable for the emulsion to be insensitive to less strongly ionizing particles, but testing is necessary in loading with desensitizing substances to evaluate the extent of this phenomenon. Adverse effects such as this may be avoided by making use of the technique described below for incorporating insoluble substances into emulsions.

Commercial Availability

Emulsions impregnated with various substances during their manufacture can be obtained from Ilford and Eastman Kodak. Ilford supplies B2, C2, and E1 emulsions loaded with either lithium or boron, and the C2 emulsions may also be supplied with bismuth loadings. Table 4–I gives the composition of Ilford loaded emulsions in grams of each element per cm^3. These figures are valid for 50 percent relative humidity at 20°C, and for significantly different humidities these values will vary somewhat. Eastman Kodak impregnate their NTA and NTB emulsions with either lithium or boron, the approximate amount of the element per cm^2 being provided with each batch. Beryllium loadings, once available, have been discontinued because of the toxicity of this element.

Deuterium Loading

Deuterium may be incorporated into nuclear emulsions by loading with calcium nitrate, $Ca(NO_3)_2$, having D_2O as water of crystallization (Gibson *et al.*, 1947). A concentration of 6 percent D_2O by weight is possible with this method. Ilford has loaded plates with the stable compound hexa-deutero-diacetin. However, much greater concentrations are obtainable by immersing emulsions directly in D_2O and exposing them while wet. In this way concentrations of from 30 to 80 percent D_2O by weight are possible. In absorbing roughly 0.5 gram D_2O per 0.2 cm^3 the emulsions swell to about 3.5 times their original thickness. The specific energy loss and range-energy curves for wet emulsions are, of course, different from those under standard conditions; Sec. 2–3 contains a discussion of the various corrections required in the case of pure water, and these results may be applied to D_2O. Although on a volumetric basis the figures for H_2O are identical with those of D_2O, the greater weight of the latter necessitates the use of an appropriate conversion factor when gravimetric measurements are employed.

Lithium Borate Loading

The various advantages of lithium and boron loading for neutron detection may be utilized simultaneously by impregnating emulsions with lithium borate ($Li_2B_4O_7$). Yagoda (1949) has given details of such impregnation. Table 4–II contains the formula for the loading bath; the boric acid is first dissolved, and a slight excess of lithium carbonate added. The solution is then cooled, filtered, and diluted to 400 ml. A 10 percent concentration of lithium borate is obtained. The glycerine plasticizer is necessary only with emulsions thicker than about 50 microns. After 15 minutes in this solution 30-micron plates absorb about 0.24-mg lithium borate per cm^2.

Uranium Loading

For investigating neutron-induced fission in uranium, uranyl nitrate or acetate solutions may be used as loading baths. San Tsiang *et al.* (1947) load 40-micron Ilford C2 emulsions for 5 minutes from a 20 percent solution, followed by immersion in ethyl alcohol and then drying in an air stream. Uranyl acetate solutions acidified with weak acetic acid were used by Green and Livesey (1948), who have determined the approximate degree of desensitization to be expected with varying concentrations. One percent unanyl acetate, for immersion times varying from 1 hour for 20-micron emulsions to 12 hours for 100-micron emulsions, gave faint proton tracks in Ilford C2 and B1 plates, distinct alpha-particle tracks and very dense fission fragment tracks. Two percent solutions rendered the plates insensitive to protons and decreased the alpha-track grain densities, while four percent solutions virtually eliminated the alpha-particle track population entirely.

Sandwiching

In impregnation a foreign substance is more or less uniformly distributed through the volume of the emulsion. In the sandwich technique, on the other hand, thin layers of the desired substances are interposed between layers of sensitive emulsions. Harding (1949), for example, has used plates consisting of alternate layers of pure gelatin and emulsion in studying cosmic radiation. Four 30-micron emulsion layers were separated by three thin ones of the gelatin. Hodgson and Perkins (1949) tried to incorporate layers of lead phosphate, also in studying cosmic rays, but the quantity of lead that can be included in this way without reducing the transparency of the processed emulsion is very small. Solid metallic foils have been used between two plates which were later separated for processing and examination (Barbour and Greene, 1950), but this method has only a limited range of application.

Insoluble Substances

It is impossible to impregnate emulsions with insoluble substances directly. However, a sandwich technique such as the one devised by Vigneron and Bogaardt (1951) permits the incorporation of solid grains in a gelatin layer between two sensitive emulsion layers. A suspension of suitably sized grains in a solution of one part gelatin to 200 parts water is first prepared, and several drops of this suspension are then spread over the surface of a nuclear emulsion. One drop is sufficient for approximately 10 cm^2 of surface area. After drying in a vacuum chamber the plate is immersed in a water bath. A second plate then is stripped of its emulsion with a razor blade, and the emulsion sheet that is obtained is placed on the first plate under water. Alternatively a pellicle may be used for this purpose. The complete sandwich, with excess moisture wiped off, is heated for four minutes at 45°C, drying being completed at reduced pressure. Plates made in this manner are extremely rugged and require no special treatment in handling or processing.

It is possible with this technique to utilize soluble elements and compounds which, if introduced as ions in solution, would alter the *p*H of the emulsion and hence its sensitivity and development characteristics. Another application especially suited for this procedure is the study of naturally and artifically radioactive substances; the origin of any track present can be identified unambiguously, and, since the grains are in the center of the emulsion sandwich, tracks emanating in any direction can be studied. Similar techniques have been employed by Demers (1946) and Picciotto (1949b, c) in their work.

TABLE 4-I. The compositions of Ilford impregnated emulsions in grams per cm^3.

Element	Lithium loaded	Boron loaded	Bismuth loaded
Silver	1.84	1.77	1.39
Bromine	1.35	1.28	1.01
Iodine	0.053	0.047	0.039
Carbon	0.27	0.26	0.33
Hydrogen	0.047	0.053	0.047
Oxygen	0.29	0.32	0.43
Sulfur	0.038	0.010	0.002
Nitrogen	0.083	0.064	0.062
Lithium	0.016	...	...
Sodium	...	0.025	0.06
Boron	...	0.023	...
Bismuth	...	...	0.27

TABLE 4-II. Formula for lithium borate loading bath.

Distilled water (hot)	300 ml
Boric acid (crystals)	60 g
Lithium carbonate	19 g
Glycerine	20 ml
Distilled water to make	400 ml

4–6. MAGNETIC DEFLECTION

The momentum of a charged particle traversing the gas of a cloud chamber is usually determined from the curvature induced in its track by a strong magnetic field. This technique is not directly applicable to nuclear emulsions, since the very short ranges of particles in the emulsion coupled with the scattering they exhibit require very high fields (perhaps 100 or more times greater than for cloud-chamber work) to produce measurable curvatures. If the deflection occurs in an air gap between two plates, however, a more reasonable field strength permits the determination of the momenta of particles passing through both plates and the intervening gap (Powell and Rosenblum, 1948; Barbour, 1948, 1950; Franzinetti, 1950, 1951; Dilworth *et al.*, 1950).

Equipment

In practice, 100- or 200-micron thickness plates are mounted rigidly in a holder several millimeters apart

(3 mm is convenient) and placed between the pole pieces of a magnet. Thicker plates would result in too great a danger of emulsion distortion during processing. To minimize distortion further the plates should be larger in area than the pole piece size so that, during drying, the useful portion of the emulsion will not be affected. A margin of about an inch is satisfactory.

It is necessary in the application of this method that the geometrical relationship of the plates during exposure be known precisely in their examination. This is conveniently accomplished by using a collimated beam of x-rays to produce a regular pattern in the mounted plates. For this purpose Barbour employs in his work a 0.03-inch lead plate with a grid of 100-micron holes spaced 0.5-cm apart and coded at intervals, while Powell's group uses a grid of thin lines (approximately 20 microns wide) formed by means of a slit in a lead plate exposed in different positions to give a regular lattice.

For permanent installations at sea level or mountain altitudes an electromagnet is suitable, as intense a field as is practicable being required for usable results. Fields as high as 27,500 gauss have been employed. Since in high altitude experiments, with aircraft or balloons, light weight is a necessity, weaker permanent magnets must be used. For balloon work a 65-pound magnet of Alnico V with a soft iron yoke and pole pieces 25.9 cm^2 in area producing a field of 13,300 gauss in a 0.25-inch gap was built by Barbour (1950) and gave satisfactory results. Magnetron magnets of several thousand gauss are commercially available, and their fields may be increased substantially by reducing their pole face areas with soft iron. The field increase is roughly inversely proportional to the reduction in area until saturation is approached, and fields of over 10,000 gauss may be obtained from such magnets in this way.

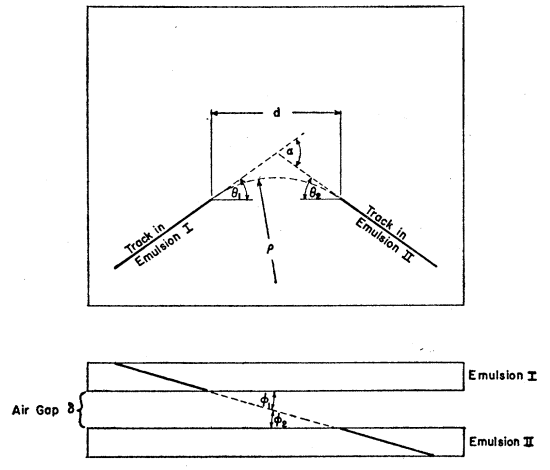

FIG. 4–6. Top and side views of plate sandwich exposed in a magnetic field showing the track of a deflected particle.

Track Analysis

In scanning the plates the locations of the various tracks are plotted on a large sheet of paper relative to the x-ray grid. The angular orientations in the emulsion plane and dip angles ϕ of the tracks must be known accurately in order to determine which pairs of tracks in the two plates are due to the same particle. A knowledge of the shrinkage factor is necessary for the evaluation of ϕ. In matching track segments the following criteria must be fulfilled:

1. The dip angles ϕ_1 and ϕ_2 (Fig. 4–6) should be equal, or very nearly so.
2. The deflection angles θ_1 and θ_2 between the continuations of the tracks and the line joining their points of entry into the air gap should agree since the path in the magnetic field is an arc of a circle.
3. The grain densities of the tracks near the emulsion surfaces should be the same. A particle loses very little energy in the air gap, and so the rates of energy loss must be equal.
4. The distance d between the points of entry of the two tracks should be consistent with the dip angles ϕ_1 and ϕ_2 and the plate separation δ.

The radius of curvature ρ of the path of the particle in the air gap may be evaluated from the equation

$$\rho=\frac{d}{2\sin\theta_1}=\frac{d}{2\sin\theta_2}. \tag{4–13}$$

However, as Barbour (1951) points out, it is preferable to use

$$\rho=d/2\sin(\alpha/2) \tag{4–14}$$

in determining ρ, since the total angular deflection α depends solely upon the difference between the measured angular orientations of the track segments. Unlike the measurements of θ, errors in the plotting angles and positions do not affect the value of α. The momentum ρ of the particle producing the track is then

$$p=eH\rho/c\cos\phi, \tag{4–15}$$

where H is the field strength, c the velocity of light, and e the charge on the electron.

It is possible to determine the mass M of the incident particle if it ends in the second emulsion, assuming unit charge. Since

$$R=Mf(v) \tag{4–16}$$

and $p=Mv$ in the nonrelativistic region, knowing both R and p permits eliminating v and calculating M. See Sec. 2–3 for details of the range-energy relationship. Barbour (1951) has given theoretical range-curvature curves in Ilford C2 emulsions for singly charged particles of several masses (Fig. 4–7), where the magnetic curvature C is defined by

$$C=(10^3\cos\phi)/H\rho. \tag{4–17}$$

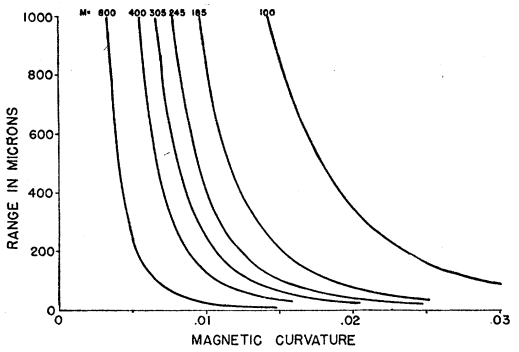

FIG. 4–7. Theoretical range-magnetic curvature plot for singly charged particles of various masses in Ilford C2 emulsions (Barbour, 1951).

The only serious errors to be encountered in this procedure, apart from those due to emulsion distortion which may be reduced to a minimum of perhaps 0.5° in the angular measurements, lie in the small angle scattering of the particle and in the determination of H. In the event of a large angle scatter in the air gaps. the particle direction would be so altered that the two track fragments could not be matched. Franzinetti (1951) has evaluated the deflection to be expected from scattering in the gap relative to the magnetic deflection, with the uncertainty in all cases being well under 4 percent. Since the scattering is proportional to the square root of the air pressure (Bethe 1946), at balloon altitudes this source of error becomes entirely negligible. It is essential, of course, that H be known accurately; but in addition, only that pole piece area may be employed which is homogeneous to at least several percent.

The possibility of two unrelated tracks in the plates being confused as parts of the same trajectory is remote for background densities of less than about 100 tracks per cm^2. Franzinetti has calculated the relative number of such spurious coincidences between a given number of tracks distributed isotropically on the two plates and obtains a value of 3.3×10^{-3} for this quantity.

4–7. MISCELLANEOUS TECHNIQUES

Scattering Cameras

Much valuable information on nuclear forces and reactions can be obtained by determining the nature and angular distribution of the particles produced or scattered when a substance is bombarded by a beam of collimated particles from an accelerator. For solid targets with which the reaction products of a nuclear process are to be investigated, plates may be placed tangentially and partially surrounding the target at an appropriate angle with the horizontal so that identifiable tracks are produced. An arrangement of this sort has been employed, for example, by Talbott *et al.* (1950) in determining the distribution of alpha-particles from the disintegration of Li^7 protons. A simplified sketch of this apparatus is given in Fig. 4–8. The known geometry of the plates during the exposure enables the conversion of the postion of every track in the emulsions to its corresponding angle of emission.

Another arrangement, with plates distributed radially around a target, was used by Wilkins (1940). In this case the particles were incident on the edges of a large number of plates, each plate providing information on a specific scattering angle. A modification of this type of camera was devised by Allred *et al.* (1951) for use with a gas target. In this case slits must be employed with each plate (Fig. 4–9) in order to define the orientation of the scattered particles with respect to the incident beam. This device, involving 69 plates, enabled simultaneous measurements to be made at 2.5° intervals over a range of 160° on either side of the beam. The angle α is, as in the case of tangentially arranged plates, a matter of experimental convenience. Other scattering cameras have been constructed for various purposes, for example by Chadwick *et al.* (1944), Rubin *et al.* (1947), May *et al.* (1947), and Rosen *et al.* (1949).

Emulsion Stacks

In cosmic-ray investigations it is usual to employ stacks of emulsions so that tracks can be followed from one plate to the next for a considerable distance under favorable conditions. A variant of this technique has been devised by Bradt and Peters (1950) in studying the heavy primary component of cosmic rays. Although grain counts give more accurate indications of specific energy loss than delta-ray determinations, their use is handicapped by the maximum ratio of specific ionizations that can be evaluated in a plate of given sensitivity. Thus if a given particle produces a barely visible track, another with about 15 times this ionizing power leaves too dense a track for grain counting. Bradt and Peters have overcome this difficulty by using stacks with alternate plates of high and low sensitivity. Eastman NTB3 and NTA plates were used, the former receiving standard processing and the latter underdevelopment through the use of 20:1 diluted D19

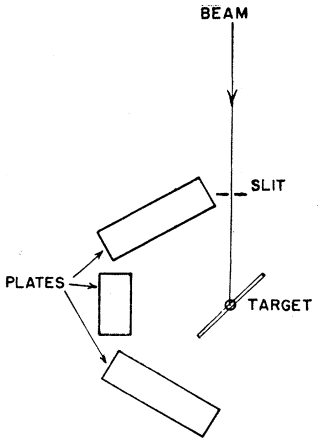

FIG. 4–8. Simplified sketch of the experimental geometry employed by Talbott *et al.* (1950) making use of tangentially arranged plates.

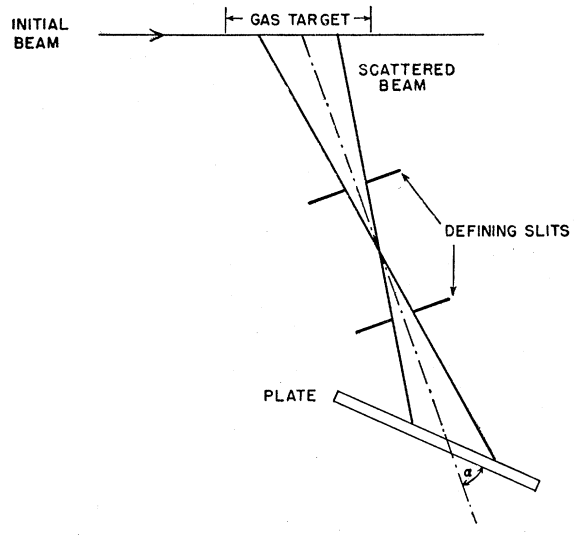

FIG. 4–9. Slit system geometry for each plate in a scattering camera using radially arranged plates (after Allred *et al.*, 1951).

developer. In Fig. 4–10 the grain densities corresponding to various specific energy losses is given in the two emulsions, with the positions on these curves of tracks due to various relativistic nuclei indicated. Ilford has just begun putting out a plate consisting of alternate layers of G5 and G0 (less sensitive) emulsion for this purpose, the G5 layers being 400 microns thick and the G0 200 microns. Preliminary results indicate that in the G0 plate the grain density in grains/100 micron is numerically equal to the energy loss in kev/micron up to a figure of 60, where saturation effects become important.

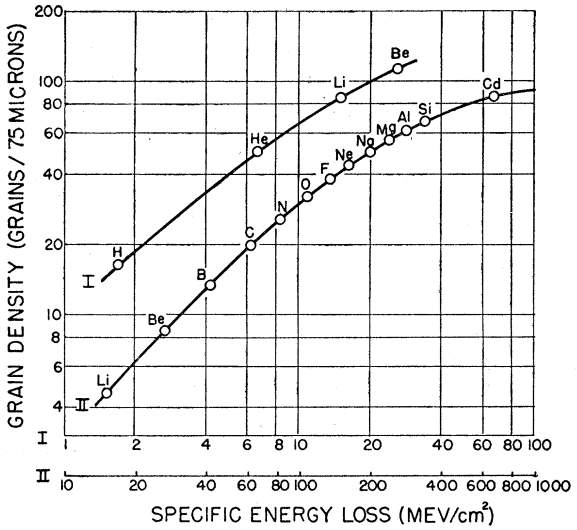

FIG. 4–10. The variation of grain density with specific energy loss in Eastman Kodak NTB3 (curve I) and NTA (curve II) emulsions. The expected grain densities of various relativistic nuclei are indicated (Bradt and Peters, 1950).

4–8. TRACK RECOGNITION

When examining emulsions with high background densities it is frequently desirable to be able to estimate the probability for finding tracks of low specific ionization. While a given plate may be sensitive to particles of energies corresponding to minimum ionization, the fog grains may nevertheless be too numerous to permit identification of their tracks. This situation is entirely analogous to the dependence of the audibility of a specific sound upon background noise. A knowledge of the variation of track visibility with both track and background grain densities is therefore useful in assessing the value of specific developed plates for various purposes.

Straight Tracks

Coates (1951) has established that the distribution of individual grains in both tracks and background is entirely random, reducing the problem of evaluating track visibility in nuclear emulsions to the more general one of evaluating the visibility of a randomly spaced line of black spots against a random background of other spots. Berriman (1951), making use of this suggestion, constructed a series of artificial fog diagrams of various densities and, by the superimposition of a number of artificial tracks each of different density, was able to determine the visibility of the latter as a function of background.

In constructing the fog diagrams tables of random numbers were used to locate the positions of the spots on sheets of graph paper, which were subsequently punched out with circular punches and the sheets then photographed against a black background. The background was assumed to consist of spherical grains of 0.2, 0.3, 0.4, and 0.6 micron diameters present in the ratios 1:4:6:4:1, respectively, and the hole sizes employed were proportional to these diameters and their relative frequencies followed the latter distribution. The diagrams increased in the number of holes punched in each by a factor of ~ 2 throughout the series, and ranged in density from the equivalent of 2×10^{-3} grain per micron^2 at 1500 diameter magnification to 500×10^{-3} grain per micron^2. The track diagrams were prepared by first constructing a track of maximum grain density and then, for the other tracks, selecting grains at random along this track until the desired density was achieved.

Two tracks of each density were superimposed simultaneously upon the backgrounds, and the maximum fog concentrations at which (1) both tracks were easily recognized and (2) only one of the tracks was recognized was determined. Condition (1) was defined as good recognition by Berriman and condition (2), approximately corresponding to an equal probability of missing as of finding the track, as fair recognition. Figure 4–11 summarizes the results that were obtained, with the minimum track densities for good and for fair recognition given as a function of the corresponding back-

ground densities. In this plot both scales are logarithmic.

The interpretation of the two inflection points in these curves is very interesting. The first, occurring at a track density of about 0.3-grain micron, is the point at which "doublets," adjacent grains that are touching each other or very nearly so, first appear. Such doublets act to increase track visibility by acting as track markers. The second inflection occurs at a background density of 0.1 grain per micron^2, and at this point the background becomes too dense to permit ready track recognition. Above this the slope of the curves increases very rapidly.

The recognition curves of Fig. 4–11 are actually underestimations of the track densities required for visibility in practice. When examining an emulsion microscopically, it is possible to investigate the regions around a field of view exhibiting a doubtful track. In addition, once the presence of a track is established, perhaps in a local area of diminished fog or because of a slightly greater grain density over a small part of its length, finding the remainder is greatly facilitated. In the artificial diagrams only the equivalent of 50-micron track segments were used. Focusing the microscope up and down during the actual scanning aids in the recognition of tracks exhibiting even a small dip angle over much denser fog backgrounds than would be thought possible from Fig. 4–11. Hence, while it is possible to accept the shapes of these curves as being approximately valid, the magnitudes involved must be interpreted as being somewhat conservative guides to track visibility.

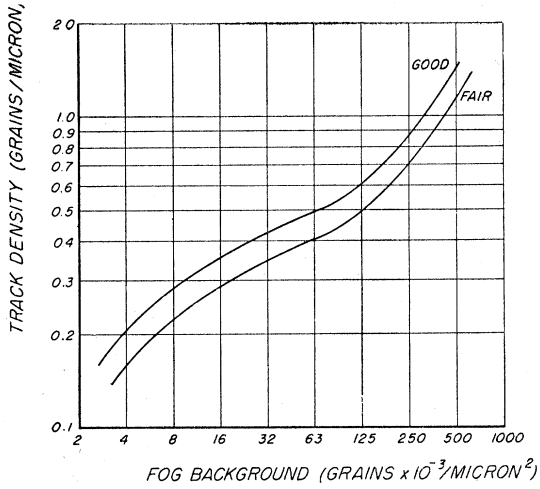

FIG. 4–11. Visibility curves of minimum track densities for recognition as a function of background density (Berriman, 1951).

Electron Track Recognition

An experiment similar to the above one was performed by Beiser (1952) with low energy electron tracks. Such tracks, unlike the ones considered by Berriman, exhibit considerable degrees of scattering and are correspondingly less easily visible. Another problem encountered was that resulting from incorrect identification of particular configurations of the random background as tracks. The background densities ranged from 1×10^{-3} to 39×10^{-3} grain per micron^2 with a common ratio of 1.5. Four reproductions of each background, three with superimposed electron track representations and one with none, were used for testing visibility. Actual 50-micron track segments were reproduced for this purpose.

In Fig. 4–12 the mean percentage probability of recognizing electron tracks is plotted as a function of background density, these results being based on a large number of individual evaluations. The criterion chosen was clear visibility; in each case the observer had to determine whether a track or tracks were present and their exact trajectories. The visibility curve shows the number of correct identifications divided by the actual number present. The other curve in Fig. 4–12, giving pseudo-track visibility, is the number of incorrect identifications divided by the actual number. It is evident that above perhaps 5×10^{-3} grain per micron^2 backgrounds a definite proportion of tracks will be missed, and that incorrect identification will become a problem. Of course, the exact value of this density is certainly less than the actual practical threshold for the reasons given above.

The decrease in slope of the visibility curve beyond 10^{-2} grain per micron^2 seems a consequence of the greater conscious care taken in the examination of dense backgrounds. The continued increase in pseudo-track recognition is also indicative of the greater concentration given, thus increasing the chance of imagining the presence of a track. It was noted that persons whose work concerns, in part at least, the distinguishing of signals (in the most general sense) over random noise were consistently superior in track recognition and made fewer incorrect identifications than others who had little or no such experience. Even experienced scanners

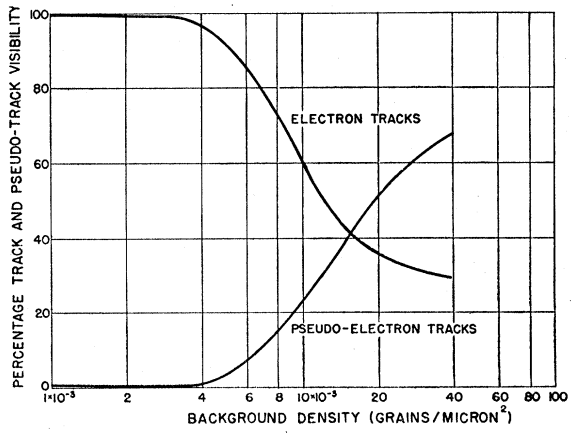

FIG. 4–12. Recognition curves as a function of background density for electron and pseudo-electron tracks in terms of the actual number present (Beiser, 1952).

were no better than, for example, people engaged in the observation of specific phenomena over noise on oscilloscope screens. A test such as this seems to have some validity in rating scanning ability, especially in so far as searching for events is concerned.

BIBLIOGRAPHY

G. Albouy and H. Faraggi, J. phys. et radium **10**, 105 (1949).
J. C. Allred, A. N. Phillips, L. Rosen, and F. K. Tallmadge, Rev. Sci. Instr. **21**, 225 (1950).
J. C. Allred, L. Rosen, F. K. Tallmadge, and J. H. Williams, Rev. Sci. Instr. **22**, 191 (1951).
Aron, Hoffman, and Williams, University of California Radiation Laboratory Report No. 121 (1949).

I. Barbour, Phys. Rev. **74**, 507 (1948).
I. Barbour, Rev. Sci. Instr. **20**, 530 (1949).
I. Barbour, Phys. Rev. **78**, 518 (1950).
I. Barbour and L. Greene, Phys. Rev. **79**, 406 (1950).
A. Beiser, Rev. Sci. Instr. **21**, 1025 (1950a).
A. Beiser, Phys. Rev. **80**, 112 (1950b).
A. Beiser, Rev. Sci. Instr. **21**, 933 (1950c).
A. Beiser, unpublished (1951a).
A. Beiser, Phys. Rev. **81**, 153 (1951b).
A. Beiser, Rev. Sci. Instr. **23**, 500 (1952).
R. W. Berriman, *Fundamental Mechanisms of Photographic Sensitivity*, J. W. Mitchell, ed. (Butterworths Scientific Publications, London, 1951), p. 272.
H. A. Bethe, Phys. Rev. **70**, 821 (1946).
P. M. S. Blackett and D. S. Lees, Proc. Roy. Soc. (London) **134**, 658 (1932).
M. Blau, Z. Physik **34**, 285 (1925).
M. Blau, Akad. Wiss. Wien **140**, 623 (1931).
M. Blau, Phys. Rev. **75**, 279 (1949).
M. Blau and J. A. De Felice, Phys. Rev. **74**, 1198 (1948).
M. Blau and H. Wambacher, Monatsh. **61**, 99 (1932).
M. Blau and H. Wambacher, Nature **134**, 538 (1934).
D. M. Bose and B. Choudhuri, Nature **147**, 240 (1941).
W. Bosley, J. D. Craggs, and W. F. Nash, Nature **161**, 1022 (1948).
H. Bradner, F. M. Smith, W. H. Barkas, and A. S. Bishop, Phys. Rev. **77**, 462 (1950).
H. L. Bradt and B. Peters, Phys. Rev. **74**, 1828 (1948).
H. L. Bradt and B. Peters, Phys. Rev. **76**, 156 (1949).
H. L. Bradt and B. Peters, Phys. Rev. **80**, 943 (1950).
H. L. Bradt, M. F. Kaplon, and B. Peters, Helv. Phys. Acta **23**, 24 (1950).
E. Broda, Nature **158**, 872 (1946).
E. Broda, J. Sci. Instr. **24**, 136 (1947).
R. Brown, U. Camerini, P. H. Fowler, H. Muirhead, C. F. Powell, and D. M. Ritson, Nature **163**, 47, 82 (1949).
W. E. Burcham and M. Goldhaber, Proc. Cambridge Phil. Soc. **32**, 632 (1936).

U. Camerini and C. M. G. Lattes, Ilford Technical Data (Ilford Ltd., London, 1947).
J. Chadwick, A. N. May, T. G. Pickavance, and C. F. Powell, Proc. Roy. Soc. (London) **183A**, 1 (1944).
J. S. Cheka, Phys. Rev. **74**, 127 (1948).
A. C. Coates, *Fundamental Mechanisms of Photographic Sensitivity*, J. W. Mitchell, ed. (Butterworths Scientific Publications, London, 1951), p. 320.
M. Cosyns, C. C. Dilworth, and G. P. S. Occhialini, Université Libre de Bruxelles Note n°6 (1949).
P. Cüer, Compt. rend. **223**, 1121 (1946).
P. Cüer, J. phys. et radium **8**, 83 (1947).
N. W. Curtis and L. S. Osborne, Phys. Rev. **75**, 1327 (1949).

A. D. Dainton, A. R. Gattiker, and W. O. Lock, Phil. Mag. **42**, 396 (1951).
R. Davies, W. O. Lock, and H. Muirhead, Phil. Mag. **40**, 1250 (1949).
P. Debye and E. Hückel, Physik. Z. **24**, 185 (1923).
P. Demers, Phys. Rev. **70**, 86 (1946).
P. Demers, Phys. Rev. **70**, 974 (1946).
P. Demers, Can. J. Research **25**, 223 (1947).
P. Demers and R. Mathieu, Phys. Rev. **75**, 1327 (1949).
C. C. Dilworth, *Cosmic Radiation*, F. C. Frank and D. R. Rexworthy, eds. (Butterworths Scientific Publications, London, 1949), p. 157.
C. C. Dilworth, S. J. Goldsack, Y. Goldschmidt-Clermont, and F. Levy, Phil. Mag. **41**, 1032 (1950).
C. C. Dilworth, G. P. S. Occhialini, and R. M. Payne, Nature **163**, 102 (1948).
C. C. Dilworth, G. P. S. Occhialini, and L. Vermaesen, Bulletin du Centre de Physique Nucleaire de L'Universite Libre de Bruxelles No. 13a (1950).
C. C. Dilworth, G. P. S. Occhialini, and L. Vermaesen, *Fundamental Mechanisms of Photographic Sensitivity*, J. W. Mitchell, ed. (Butterworths Scientific Publications, London, 1951), p. 297.
E. M. Dollmann, Rev. Sci. Instr. **21**, 118 (1950).

B. T. Feld, Massachusetts Institute of Technology Laboratory for Nuclear Science and Engineering Technical Report No. 8 (1948).
P. H. Fowler, Phil. Mag. **41**, 169 (1950).
P. H. Fowler and D. H. Perkins, *Fundamental Mechanisms of Photographic Sensitivity*, J. W. Mitchell, ed. (Butterworths Scientific Publications, London, 1951), p. 340.
C. Franzinetti, Phil. Mag. **41**, 86 (1950).
C. Franzinetti, *Fundamental Mechanisms of Photographic Sensitivity*, J. W. Mitchell, ed. (Butterworths Scientific Publications, London, 1951), p. 159.
P. Freier, E. J. Lofgren, E. P. Ney, F. Oppenheimer, H. L. Bradt, and B. Peters, Phys. Rev. **74**, 213 (1948a).
P. Freier, E. J. Lofgren, E. P. Ney, and F. Oppenheimer, Phys. Rev. **74**, 1818 (1948b).
D. Froman, L. Rosen, and B. Rossi, Bull. Am. Phys. Soc. **22**, No. 3, p. 5 (1947).

W. M. Gibson and D. L. Livesey, Proc. Phys. Soc. (London) **60**, 523 (1948).
W. M. Gibson, L. L. Green, and D. L. Livesey, Nature **160**, 534 (1947).
E. Glückauf and F. A. Paneth, Proc. Roy. Soc. (London) **165A**, 229 (1938).
G. Goldhaber, Phys. Rev. **74**, 1725 (1948).
G. Goldhaber, Phys. Rev. **77**, 753 (1950).
Y. Goldschmidt-Clermont, Nuovo cimento **7**, 33 (1950).
Y. Goldschmidt-Clermont, D. T. King, H. Muirhead, and D. M. Ritson, Proc. Phys. Soc. (London) **61**, 183 (1948).
K. Gottstein, M. G. K. Menon, J. H. Mulvey, C. O'Cealleigh, and O. Rochat, Phil. Mag. **42**, 708 (1951).
L. L. Green and D. L. Livesey, Nature **158**, 272 (1946).
L. L. Green and D. L. Livesey, Proc. Cambridge Phil. Soc. **241A**, 223 (1948).
J. C. Grosskreutz, Phys. Rev. **76**, 482 (1949).
R. W. Gurney and N. F. Mott, Proc. Roy. Soc. (London) **164A**, 151 (1938).

W. Hälg and L. Jenny, Helv. Phys. Acta **21**, 131 (1948).
D. Halliday, *Introductory Nuclear Physics* (John Wiley and Sons, Inc., New York, 1950).
H. Hänni, V. L. Telegdi, and W. Zünti, Helv. Phys. Acta **21**, 203 (1948).
J. B. Harding, Nature **163**, 440 (1949).
A. Hautot, Sci. Ind. Phot. (2) **19**, 441 (1948).
R. H. Herz, Phys. Rev. **75**, 478 (1949).
P. E. Hodgson and D. H. Perkins, Nature **163**, 439 (1949).
P. V. C. Hough, Phys. Rev. **76**, 163 (1949).
P. V. C. Hough, Phys. Rev. **80**, 1069 (1950).

A. Jdanoff, J. phys. et radium **6**, 233 (1935).
L. Jenny, *Fundamental Mechanisms of Photographic Sensitivity*, J. W. Mitchell, ed. (Butterworths Scientific Publications, London, 1951), p. 259.

H. Kallmann, Research **1**, 254 (1948).
G. R. Keepin and J. H. Roberts, Phys. Rev. **76**, 154 (1949).
G. R. Keepin and J. H. Roberts, Rev. Sci. Instr. **21**, 163 (1950).
S. Kinoshita, Proc. Roy. Soc. (London) **83**, 432 (1910).
F. H. Krenz, Proceedings of the Conference on Nuclear Chemistry, Ottawa (1947), p. 192.
V. E. Krohn and E. F. Schrader, Case Institute of Technology Nuclear Physics Laboratory Technical Report No. 8 (1951).

J. LaPalme and P. Demers, Phys. Rev. **72**, 536 (1947).
K. Lark-Horovitz and W. A. Miller, Phys. Rev. **59**, 941 (1941).
C. M. G. Lattes, P. H. Fowler, and P. Cüer, Nature **159**, 301 (1947a).
C. M. G. Lattes, P. H. Fowler, and P. Cüer, Proc. Phys. Soc. (London) **59**, 883 (1947b).
C. M. G. Lattes and G. P. S. Occialini, Nature **159**, 331 (1947).
C. M. G. Lattes, G. P. S. Occhialini, and C. F. Powell, Nature **160**, 486 (1947c).
C. M. G. Lattes, G. P. S. Occhialini, and C. F. Powell, Proc. Phys. Soc. (London) **61**, 173 (1948).
S. Lattimore, Nature **161**, 518 (1948).
D. L. Livesey and D. H. Wilkinson, Proc. Roy. Soc. (London) **195A**, 123 (1948).
M. S. Livingston and H. A. Bethe, Revs. Modern Phys. **9**, 245 (1937).
J. J. Lord, Phys. Rev. **81**, 901 (1951).

K. B. Mather, J. Opt. Soc. Am. **38**, 1054 (1948).
K. B. Mather, Phys. Rev. **76**, 486 (1949).
P. B. Mauer and H. L. Reynolds, Phys. Rev. **73**, 1131 (1948).
A. N. May and C. F. Powell, Proc. Roy. Soc. (London) **190A**, 170 (1947).
C. E. K. Mees, *The Theory of the Photographic Process* (Macmillan, New York, 1942).
W. Michl, Akad. Wiss. Wien **121**, 1431 (1912).
C. H. Millar, A. G. W. Cameron, and M. Glicksman, Can. J. Research **28A**, 475 (1950).
J. W. Mitchell, Sci. Ind. Phot. **19**, 361 (1948).
J. W. Mitchell, Phil. Mag. **40**, 249 (1949a).
J. W. Mitchell, Phil. Mag. **40**, 667 (1949b).
G. Molière, Z. Naturforsch. **2a**, 133 (1947).
G. Molière, Z. Naturforsch. **3a**, 78 (1948).
M. Morand and L. van Rossum, *Fundamental Mechanisms of Photographic Sensitivity*, J. W. Mitchell, ed. (Butterworths Scientific Publications, London, 1951), p. 317.
M. Mortier and L. Vermaesen, Centre de Physique Nucleaire de Bruxelles Note No. 5 (1948).
N. F. Mott, Proc. Roy. Soc. (London) **124**, 425 (1929).
L. Myssowsky and P. Tschijow, Z. Physik **44**, 408 (1927).

N. Nereson and F. Reines, Rev. Sci. Instr. **21**, 534 (1950).

N. A. Perfilov, Compt. rend. U.S.S.R. **42**, 258 (1944a).
N. A. Perfilov, Compt. rend. U.S.S.R. **43**, 14 (1944b).
E. Picciotto, Compt. rend. **228**, 173 (1949a).
E. Picciotto, Compt. rend. **228**, 2020 (1949b).
E. Picciotto, Compt. rend. **229**, 117 (1949c).
E. Pickup, Phys. Rev. **74**, 495 (1948).
C. F. Powell, Nature **145**, 155 (1940).
C. F. Powell, Proc. Roy. Soc. (London) **181A**, 344 (1943).
C. F. Powell and F. C. Champion, Proc. Roy. Soc. (London) **183A**, 64 (1944).
C. F. Powell, G. P. S. Occhialini, and D. L. Livesey, J. Sci. Instr. **23**, 102 (1946).
C. F. Powell and G. P. S. Occhialini, *Nuclear Physics in Photographs* (Oxford University Press, London, 1947).
C. F. Powell and S. Rosenblum, Nature **161**, 473 (1948).

M. Reingamum, Physik. Z. **12**, 1076 (1911).
F. A. Roads, *Fundamental Mechanisms of Photographic Sensitivity*, J. W. Mitchell, ed. (Butterworths Scientific Publications, London, 1951), p. 327.
L. Rosen, F. K. Tallmadge, and J. H. Williams, Phys. Rev. **76**, 1283 (1949).
M. A. S. Ross and B. Zajac, Nature **162**, 923 (1948).
J. Rotblat, Nature **165**, 387 (1950).
J. Rotblat, *Progress in Nuclear Physics I*, O. R. Frisch, ed. (Butterworth-Springer Ltd., London, 1950), p. 37.
J. Rotblat and C. T. Tai, Nature **164**, 835 (1949).
J. Rotblat and C. T. Tai, *Fundamental Mechanisms of Photographic Sensitivity*, J. W. Mitchell, ed. (Butterworths Scientific Publications, London, 1951), p. 331.
S. Rubin, W. A. Fowler, and C. C. Lauritsen, Phys. Rev. **71**, 212 (1947).
E. Rutherford, Phil. Mag. **47**, 277 (1924).

T. San Tsiang, Ho Zah Wei, R. Chastel, and L. Vigneron, J. phys. et radium **8**, 1, 26 (1947).
M. M. Shapiro, Revs. Modern Phys. **13**, 58 (1941).
S. F. Singer, Office of Naval Research (London) Technical Report No. 71 (1951).
J. H. Smith, Phys. Rev. **71**, 32 (1946).
H. S. Snyder and W. T. Scott, Phys. Rev. **76**, 220 (1949).
P. H. Stelson, Massachusetts Institute of Technology Laboratory for Nuclear Science and Engineering Technical Report No. 47 (1950).
B. Stiller, private communication (1951).
B. Stiller, M. M. Shapiro, and F. W. O'Dell, Bull. Am. Phys. Soc. **26**, No. 6, 16 (1951).

F. L. Talbott, A. Busala, and G. C. Weiffenbach, Catholic University of America Technical Report No. 1 (1950).
H. J. Taylor, Proc. Roy. Soc. (London) **150**, 382 (1935).

S. von Friesen and K. Kristiansson, Nature **166**, 686 (1950).
L. van Rossum, J. phys. et radium **10**, 402 (1949).
L. Vigneron, J. phys. et radium **10**, 305 (1949).
L. Vigneron and M. Bogaardt, *Fundamental Mechanisms of Photographic Sensitivity*, J. W. Mitchell, ed. (Butterworths Scientific Publications, London, 1951), p. 265.

H. Wäffler and S. Younis, Helv. Phys. Acta **22**, 414 (1949).
H. Wambacher, Z. wiss. Phot. **38**, 38 (1939).
J. H. Webb, Phys. Rev. **74**, 511 (1948).
J. Wheeler and R. Ladenburg, Phys. Rev. **60**, 754 (1941).
M. Weiner and H. Yagoda, Rev. Sci. Instr. **21**, 39 (1950).
T. R. Wilkins, J. Appl. Phys. **11**, 35 (1940).
E. J. Williams, Proc. Roy. Soc. (London) **169A**, 531 (1939).
E. J. Williams, Phys. Rev. **58**, 292 (1940).
M. J. Wilson and S. Vaneslow, Phys. Rev. **75**, 1144 (1949).
L. Winand and L. Falla, Bull. Soc. Sci. Liège **18**, 184 (1949).

H. Yagoda, *Radioactive Measurements with Nuclear Emulsions* (John Wiley and Sons, Inc., New York, 1949).
H. Yagoda and N. Kaplan, Phys. Rev. **71**, 910 (1947).
H. Yagoda and N. Kaplan, Phys. Rev. **73**, 634 (1948).
P. K. S. Yang and M. Weiner, Phys. Rev. **76**, 1724 (1949).